Oncology and Translational Medicine

Volume 2 • Number 3 • June 2016

Oncology and Translational Medicine Volume 2 • Number 3 • June 2016 pp 97–141

邮发代号：38-121
ISSN 2095-9621

GENERAL INFORMATION
≫otm.tjh.com.cn

ISSN 2095-9621
CN 42-1865/R

Oncology and Translational Medicine

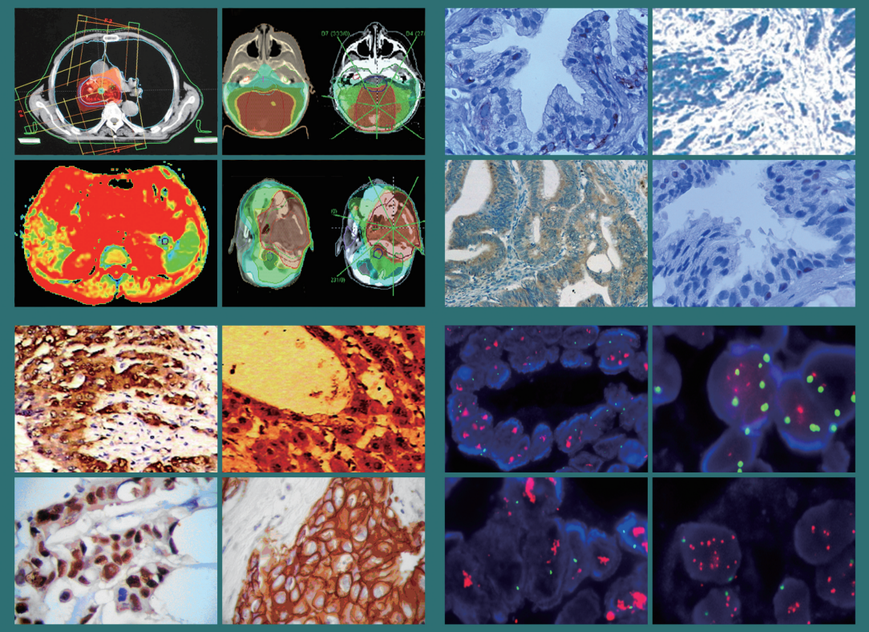

Volume 2
Number 3
June 2016

Oncology and Translational Medicine

Oncology and Translational Medicine
June 2016 Volume 2 Number 3

Contents

Oncology and Translational Medicine
DOI 10.1007/s10330-016-0161-9
June 2016, Vol. 2, No. 3, P97–P98

EDITORIAL

Progress in the molecular pathology of glioma

Changshu Ke (✉)

Department of Pathology, Tongji Hospital, Tongji Medical College, Huazhong University of Science and Technology, Wuhan 430030, China

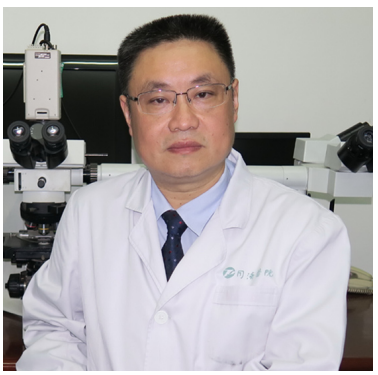

Changshu Ke, Associate Professor of Pathology, Masters Supervisor, Associate Director of the Department of Pathology, Tongji Hospital, Tongji Medical College of HUST, China. Prof. Ke graduated from The Fourth Military Medical University in 1986 and obtained his Master's degree in the Department of Pathology, PLA General Hospital (Beijing), in 1989. In 1995, he received a fellowship for training in surgical pathology supported by the Hong Kong Division of the International Association of Pathology, which was held at the Department of Anatomical and Cellular Pathology, Prince of Wales Hospital, The Chinese University of Hong Kong. From 1997 to 2001, he studied in the Faculty of Medicine, The Chinese University of Hong Kong, and obtained his doctorate in 2001. He is now in charge of clinical services at the Department of Pathology, Tongji Hospital, Tongji Medical College, HUST. In addition, he teaches the pathology courses for medical students, and overseas medical students and graduate students (neuropathology courses). His research is mainly focused on brain edema, the surgical pathology of CNS tumors, and experimental studies in tumor biology. His current academic activities include: member of the editorial board of the Chinese Journal of Clinical Neurosurgery, member of the Neuropathology Group of the Pathological Society of the Chinese Medical Association, member of the Standing Committee of Onco-pathology Specialty of Chinese Anti-Cancer Association, and vice chairman of the Standing Committee of Onco-pathology Specialty of Hubei Anti-Cancer Association.

Glioma represents the most common primary tumor in the central nervous system (CNS). Along with the increased incidence of brain tumors, there was a 194% increase in brain tumor-related mortality in China in 2008 compared with that of the 1970s [1]. Malignant glioma, as the main pathological subtype of brain tumor, often leads to a fatal outcome because of its invasive nature and resistance to currently available treatments, posing great challenges to public health.

For the past century, the classification and pathological diagnosis of glioma has been primarily based on microscopic morphology, including analysis of hematoxylin and eosin-stained slides, immunohistochemical staining, and ultrastructural features, when compared with the putative cells of histogenesis and their presumed differentiation. According to the World Health Organization (WHO) classification of CNS tumors (2007 edition), glioma can be divided into four grades: Grade I (benign), Grade II (low malignant potential), Grade III (malignancy), and Grade IV (high-grade malignancy). The last two decades of molecular research have provided valuable and encouraging information about tumorigenesis. Along with the development and accumulation of molecular pathological data, it is now possible to define different entities of glioma, and other brain tumors, by integrating both histological and molecular parameters, as introduced in the updated WHO Classification of CNS tumors (2016 edition) [2]. In this new classification, the diffuse gliomas include astrocytic tumors (Grades II & III), oligodendrogliomas (Grades II & III), glioblastoma (Grade IV), as well as diffuse glioma in children, presenting the molecular phenotypes of the IDH-mutant, IDH-wild type, and NOS categories. Other astrocytomas with distinct genetic features usually show a circumscribed tumor margin, lack *IDH* gene alterations, and bear the frequent *BRAF* gene alterations (seen in pilocytic astrocytoma, pleomorphic xanthastrocytoma) and the *TSC1/TSC2* mutation (seen in subependymal giant cellastrocytoma), etc. The previous astrocytoma entities protoplasmic astrocytoma and fabrillary astrocytoma were abandoned because of their overlapping genetic characteristics. The entity "gliomatosis cerebri" has also been removed, which has been considered as one of the most widespread invasive tumor growth patterns consistently observed in many diffuse

✉ Correspondence to: Changshu Ke. Email: kecs@hust.edu.cn

astrocytomas. Glioblastoma can be divided into glioblastoma with the IDH-wild type (*de novo* variant) and glioblastoma with the IDH-mutant (secondary variant). Furthermore, the diagnosis of oligodendroglioma and anaplastic oligodendroglioma now requires screening for *IDH* mutation and 1p/19q co-deletion. In ependymoma and anaplastic ependymoma, only one genetic subtype was accepted: RELA fusion-positive subtype.

There are several intracellular signaling pathways of focus in glioma research, because of their important roles in glioma cell growth and maintenance of malignancy, including the receptor tyrosine kinase/Ras/phosphatidylinositol 3-kinase pathway, TP53 pathway, and RB pathway [3]. In the angiogenesis of gliomas, the related signaling pathways include upregulation of angiopoietin-2 (ANG-2)/tyrosine kinase with immunoglobulin-like and epidermal growth factor homology (TIE-2), promotion of vessel disruption, followed by vascular endothelial growth factor (VEGF) binding to the VEGF receptor (VEGFR), which activates intracellular signaling cascades transduced by the RAS/MAPK and PI3K/AKT pathways, leading to enhanced proliferation of endothelial cells. This detailed information of signaling pathways has now made it possible to select and design molecular targeted therapy of gliomas.

In general, the molecular pathology of gliomas has progressed considerably within the last two decades, highlighting the bright future of the application of molecular technology in clinical and experimental research on gliomas. It is reasonable to hope that the integration of histopathological and molecular parameters in glioma diagnosis and classification may help to reveal more information of the biology of human gliomas and the impact on molecular targeted therapy; meanwhile, this progress is expected to motivate and inspire a new generation of investigators in this field.

References

1. Hou L, Jiang J, Liu B, *et al*. Smoking and adult glioma: a population-based case-control study in China. Neuro Oncol, 2016, 18: 105–113.
2. Louis DN, Perry A, Reifenberger G, *et al*. The 2016 World Health Organization Classification of Tumors of the Central Nervous System: a summary. Acta Neuropathol, 2016, 131: 803–820.
3. Wang H, Xu T, Jiang Y, *et al*. The challenges and the promise of molecular targeted therapy in malignant gliomas. Neoplasia, 2015, 17: 239–255.

DOI 10.1007/s10330-016-0161-9
Cite this article as: Ke CS. Progress in the molecular pathology of glioma. Oncol Transl Med, 2016, 2: 97–98.

Oncology and Translational Medicine
DOI 10.1007/s10330-016-0135-y

June 2016, Vol. 2, No. 3, P99–P103

REVIEW ARTICLE

Epidermal growth factor receptor: a key manipulator in molecular pathways of malignant glioma

Changshu Ke (✉)

Department of Pathology, Tongji Hospital, Tongji Medical College, Huazhong University of Science and Technology, Wuhan 430030, China

Abstract

The epidermal growth factor receptor (EGFR) is a member of the ErbB/EGFR family, including EGFR/Her1, ErbB2/Her2, ErbB-3/Her3, and ErbB-4/Her4. EGFR exerts its effects through the receptor tyrosine kinase phosphorylation and activation of important downstream signaling pathways in normal and neoplastic cells, mainly the Ras GTPase/MAP kinase (MAPK), STAT3, and phosphatidylinositide 3 kinase-AKT pathways. EGFR deregulation is common in malignant glioma, especially primary glioblastoma, and exists in three forms: gene overexpression (amplification), autocrine effects of EGFR activation, and activating receptor mutation (EGFRvIII). However, some EGFR abnormalities have also been found in low-grade gliomas, including the nuclear localization of EGFR, expression in the microfoci of anaplastic transformation, and association with neovascularization in the mesenchyma of the glioma, which suggests that some unknown EGFR-related mechanisms are possibly responsible for its central role in the initiation and progression of malignant glioma. Uncovering these mechanisms will have potential value in the development of radiotherapy, chemotherapy, and EGFR-targeted therapy for glioma.

Received: 25 January 2016
Revised: 19 February 2016
Accepted: 25 March 2016

Key words: epidermal growth factor receptor (EGFR); molecular pathways; malignant glioma

Gliomas represent the largest group (accounting for about 40%) of primary central nervous system (CNS) tumors, representing approximately 2% of all systemic tumors in adults. According to the World Health Organization (WHO) CNS tumor classification (2007), gliomas can currently be classified into distinct subtypes, mainly: pilocytic astrocytoma, diffuse glioma (astrocytoma, oligodendroglioma, ependymoma), anaplastic gliomas, and glioblastoma (GBM), based on their clinical, histopathological, and molecular characteristics. The grading system of CNS tumors is also stratified according to their biological behavior, from Grade I to IV. For example, Grade I refers to benign biological behavior, and Grades II, III, and IV denote behavior with malignant potential, malignancy, and high-grade malignancy, respectively. The gliomas (Grades II–IV) all show malignant biological behavior, and are therefore commonly known as malignant gliomas [1–3].

Although consistent efforts are focused on understanding the pathogenesis, progression, and therapeutics of malignant gliomas, these factors pose significant challenges to clinicians. However, recent understanding of CNS tumors has been revolutionized by a series of genomic studies [4–5]. For example, mutations in the isocitrate dehydrogenase (IDH1/2) gene are thought to occur early in gliomagenesis and are associated with tumor progression; although these mutations are found in 70–80% of Grade II and III gliomas and secondary GBMs, they rarely occur in primary GBM [6–7]. Loss-of-expression mutations of the alpha-thalassemia/mental retardation syndrome X-linked (ATRX) gene has a similar distribution pattern in gliomas as the IDH mutations, which possibly lead to a better prognosis [8]. Malignant gliomas bearing the 1p and 19q co-deletion are associated with longer survival, however, a glioma of the same grade but without such genetic alteration could not be differentiated histopathologically [9]. The expression of FOXG1 is notably higher in glioma tissues than in the control brain tissues, and is positively correlated with histological malignancy [10]. In addition, the O^6-methylguanine-DNA methyltransferase methylation, v-RAF murine sarcoma viral oncogene homolog B1 (BRAF) alterations, and TP53 mutation were commonly found in low-grade astrocytomas. Mutations of telomerase reverse transcriptase (TERT) have been found in ma-

✉ Correspondence to: Changshu Ke. Email: kecs@hust.edu.cn

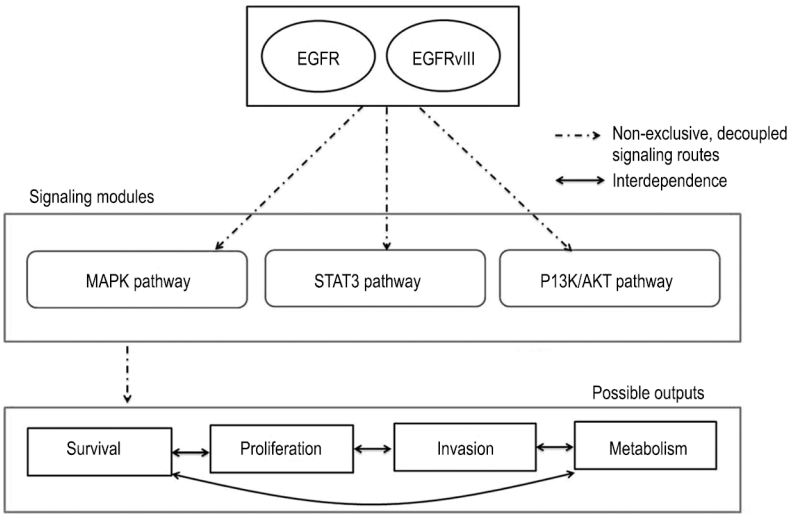

Fig. 1 Examples of modularity in the EGFR-driven signaling system

jority of the primary GBMs, but are less common in lower-grade gliomas and secondary GBMs [11–12]. Epidermal growth factor receptor (EGFR) variant III (EGFRvIII) was found in 20–30% of the GBMs [13]. As described above, identification of a series of driver mutations in gliomas has broadened our understanding of the field, thus, helping to better assess the prognosis of patients, revealing new insights into gliomagenesis, and establishing possible and specific strategies for molecular-targeted treatment in future.

EGFR (ErbB-1; HER1 in humans) is the cell-surface receptor for members of the epidermal growth factor (EGF) family. The EGFR gene is located at chromosome 7p11.2, encoding 1186 amino acid residues with a molecular weight of 170 KDa. EGFR belongs to the ErbB family of receptors, along with three related receptor tyrosine kinases: HER2/c-neu (ErbB-2), Her3 (ErbB-3), and Her4 (ErbB-4) [14–15]. EGFR is activated by binding of its main ligands, EGF and transforming growth factor-α (TGFα), as well as with some other ligands, including amphiregulin, epigen, heparin-binding EGF-like growth factor, epiregulin, and betacellulin. The ligand binding results in an active dimeric conformation of EGFR (homodimerization/heterodimerization). Subsequently, the catalytic intracellular domain is activated by phosphorylation of tyrosine residues, and proteins containing an Src homology domain 2 (SH2) region recognize the tyrosine phosphate residues and bind directly to the activated receptor. Such proteins then become activated and transfer the signal to downstream effectors [16] through the Ras GTPase/MAP kinase (MAPK), STAT3, and phosphatidylinositide 3 kinase (PI3K)-AKT pathways (Fig. 1) [17].

Along with the activation of these molecular pathways, DNA synthesis and cell proliferation are initiated, and receptor tyrosine phosphorylation also simultaneously initiates the recruitment of ubiquitin ligases as a negative regulatory mechanism [18]. Since the essential role of EGFR in epithelial development was discovered, mutations leading to EGFR over-expression have been associated with a number of neoplasms, including lung cancer, anal cancer, breast cancer, and GBM. Somatic mutations of EGFR usually result in constant activation, leading to uncontrolled cell division. Mutations, amplifications, or misregulations of EGFR or family members are detected in about 30% of all human epithelial cancers.

There are three main mechanisms of the deregulation of EGFR. The first mechanism is EGFR overexpression, and increased EGFR abundance is found in primary GBM through gene amplification and/or increased translation of this gene. Amplification of the EGFR gene has been reported in 40–70% of primary GBMs [19–20], implicating its possible role in driving gliomagenesis in primary GBMs, although some cases of GBM with EGFR overexpression without amplification have been reported [21]. The second mechanism of EGFR deregulation is an autocrine mechanism. EGFR overexpression is sometimes accompanied with an increased abundance of its cognate ligands such as EGF and TGF-α, forming uncontrolled autocrine cycles, resulting in long-lasting EGFR signal activation [22]. The third mechanism is through activating receptor mutations. Among these, 20–30% of primary GBMs express a variant mutation form of EGFR, EGFRvIII, due to the deletion of exons 2–7, which results in a constitutively active receptor that is unable to bind to a ligand and leads to continuous activation of cell growth and anti-apoptotic pathways [13]. Activation of EGFR in gliomas also occurs through gain-of-function mutations and via double minute chromosomes [23]. One study also demonstrated that a cell line stably expressing EGFRvIII and EGFL858R displayed decreased growth and migration ability compared with wild type EGFR-expressing cells, suggesting that there are distinct functional differences between differ-

ent EGFR mutation forms. The functional differences between different mutations highlight the necessity for the development of mutation-specific targeted therapies [24]. The Cancer Genome Atlas consortium identified EGFR as the fourth most highly mutated gene based on the results from a cohort of 91 GBM cases [25]. The mutation forms of EGFR may occur at the extracellular domains (EGFRvI and EGFRvII) and/or at the intra-cytoplasmic tail of the receptor (EGFRvIV, EGFRvV) [26–30]. The most frequent EGFRvIII mutation form is mainly observed in GBMs, with a much lower incidence in non-small cell carcinoma and other human cancers [30–32]. The oncogenic mechanism of EGFR mutant forms involves a series of signaling networks. For example, defects in receptor internalization result in its constitutive localization to the plasma membrane and sustained unattenuated signals [33]; phosphorylation of EGFRvIII induces a stable increase in the phosphorylation level that is distinct from that in the wild type EGFR [34]; activation of the PI3K pathway, which is negatively regulated by phosphoinositide phosphatases, including Src homology 2 domain-containing inositol phosphatases (SHIP-1 and -2); through the Erk1/Erk2 MAPK pathway by receptor dimerization, EGFR transphosphorylation, and activation, which are triggered by Grb2 binding directly to the receptor at residue Y1068 and indirectly through Src homology domain-containing adaptor protein C binding at residues Y1173 and Y1148 of the EGFRvIII mutant [35]; or through the signal transducer and activator of transcription (STAT) pathway. STAT proteins are a family of latent transcription factors that are recruited to ligand-bound EGFR dimers in combination with SH2 domains. The kinase domain of EGFR may phosphorylate the STATs, inducing their homo- or heterodimers, via SH2-phosphotyrosine interactions [36–37] and exert biological effects by colocalization of EGFRvIII and STAT3 in the nucleus of glioma cells [38]. Considering the important role of EGFR and related molecular pathways, the possibility of a new molecular classification of gliomas based on EGFR and platelet-derived growth factor receptor A (PDGFRA) expression has been recently explored [39]. EGFR-related molecular pathways are considered to play a key role in the poor prognosis of gliomas. Gene coexpression modules around EGFR (EM, 29 genes) or PDGFRA (PM, 40 genes) in 1369 adult diffuse gliomas (WHO Grades II–IV) were examined. Based on the EM and PM expression signatures, three subtypes were categorized: EM, PM, and EM (low) PM (low) gliomas, in a morphology-independent manner. Besides their distinct patterns of genomic alterations, EM gliomas were found to be associated with old age, poor prognosis, and strong expression of neural stem cell and astrogenesis genes. The EM/PM-based molecular classification scheme is applicable to adult low-grade and high-grade diffuse gliomas, and outperforms existing classification schemes in assigning diffuse gliomas to subtypes with distinct transcriptomic and genomic profiles. This EM/PM-based molecular classification provides a new molecular diagnostic framework to improve our current knowledge on the biology of malignant glioma.

It is generally recognized that EGFR abnormality is seldom found in low-grade gliomas; however, these have nevertheless been reported in several studies. In a group of 145 glioma cases, including pilocytic astrocytoma, astrocyma, anaplastic astrocytoma, and GBM cases, Carvalho *et al* [40] demonstrated EGFR overexpression and EGFR amplification in 50% and 20% of astrocytomas, respectively, whereas the EGFRvIII mutation was only found in GBMs (34.5%, $P = 0.005$). Among EGFR-amplified GBM cases, 59% also showed EGFRvIII expression ($P < 0.001$). Furthermore, cytoplasmic accumulation of EGFR protein was also found in 75% of astrocytomas detected by immunohistochemistry, and 21% of the astrocytomas showed nuclear localization of EGFR. The detection of EGFR alterations in all grades of astrocytoma implicates its key role in the progression of gliomas. In addition, Pedeutour-Braccini *et al* [41] evaluated a group of Grade II gliomas to search for high-grade glioma components within the Grade II tumor tissue; microfoci with high cellular density, high vascular density, or minimal endothelial proliferation were determined, which were referred to as the GII+ phenotype. Furthermore, cell proliferation, hypoxia, vascularization, and alterations of tumorigenic pathways were examined in the hypercellular foci of 16 GII+ cases by immunohistochemistry of Ki-67, CD31, HIF-1-alpha, EGFR, P-AKT, P53, and MDM2, and with fluorescence *in situ* hybridization of EGFR, MDM2, and PDGFRA. Ki-67 and CD31 expression was higher in the foci than in the tumor background in all cases. Aberrant expression of protein markers and genomic aberrations were also observed in some foci, and EGFR overexpression was detected in 7/16 cases, which was distinct from the tumor background. Survival of patients was shorter among GII+ cases than for all GII cases. These foci were thought to be an early histological hallmark of anaplastic transformation, which is supported by molecular aberrations. Further molecular analysis is needed to elucidate the pathogenesis of low-grade glioma progressing to high-grade glioma.

Besides the genetic abnormality of EGFR in the glioma parenchyma, the neovascularization of the glioma interstitia is also related to EGFR mutation. A recent study [42] using the LN229 GBM cell line transfected with EGFR wild type and EGFRvIII mRNA showed upregulation of the mRNA and protein expression levels of angiopoietin-like 4 factor by EGFRvIII overexpression. However, knockdown of this factor using shRNA significantly decreased the microvascular density in the transplanted tumor and inhibited its growth both *in vitro* and *in vivo*.

Further work demonstrated that the ERK pathway and its downstream regulated c-Myc pathway may be responsible for these effects.

In the last decade of molecular biological research, there have been many crucial findings relevant to gliomas, including the discovery that many of the genes involved in the initiation and progression of malignant gliomas are involved in EGFR signaling networks, which in turn govern the rampant tumor proliferation, invasive growth, and microvascular hyperplasia. Along with clinical applications of next-generation sequencing [43], the picture of the molecular pathogenesis and progression of malignant gliomas will undoubtedly become clear, with the hope of generating new pathways for drug or biomarker development to treat malignant gliomas in the future.

Conflicts of interest

The authors indicated no potential conflicts of interest.

References

1. Choi BD, Archer GE, Mitchell DA, *et al*. EGFRvIII-targeted vaccination therapy of malignant glioma. Brain Pathol, 2009, 19: 713–723.
2. Appin CL, Brat DJ. Molecular pathways in gliomagenesis and their relevance to neuropathologic diagnosis. Adv Anat Pathol, 2015, 22: 50–58.
3. Louis DN, Ohgaki H, Wiestler OD, *et al.* (eds) WHO Classification of Tumours of the Central Nervous System. Lyon: IARC Press, 2007. 13–93.
4. Wang J, Bettegowda C. Genomic discoveries in adult astrocytoma. Curr Opin Genet Dev, 2015, 30: 17–24.
5. Siegal T. Clinical impact of molecular biomarkers in gliomas. J Clin Neurosci, 2015, 22: 437–444.
6. Watanabe T, Nobusawa S, Kleihues P, *et al.* IDH1 mutations are early events in the development of astrocytomas and oligodendrogliomas. Am J Pathol, 2009, 174: 1149–1153.
7. Parsons DW, Jones S, Zhang X, *et al*. An integrated genomic analysis of human glioblastoma multiforme. Science, 2008, 321: 1807–1812.
8. Jiao Y, Killela PJ, Reitman ZJ, *et al.* Frequent ATRX, CIC, FUBP1 and IDH1 mutations refine the classification of malignant gliomas. Oncotarget, 2012, 3: 709–722.
9. Wick W, Hartmann C, Engel C, *et al*. NOA-04 randomized phase III trial of sequential radiochemotherapy of anaplastic glioma with procarbazine, lomustine, and vincristine or temozolomide. J Clin Oncol, 2009, 27: 5874–5880.
10. Shao ZW, Cong BB, Sui AH, *et al*. Expression of FOXG1 is associated with the malignancy of human glioma. Oncol Transl Med, 2014, 13: 594–599.
11. Nonoguchi N, Ohta T, Oh JE, *et al.* TERT promoter mutations in primary and secondary glioblastomas. Acta Neuropathol, 2013, 126: 931–937.
12. Killela PJ, Reitman ZJ, Jiao Y, *et al*. TERT promoter mutations occur frequently in gliomas and a subset of tumors derived from cells with low rates of self renewal. Proc Natl Acad Sci USA, 2013, 110: 6021–6026.
13. Gan HK, Kaye AH, Luwor RB. The EGFRvIII variant in glioblastoma multiforme. J Clin Neurosci, 2009, 16: 748–754.
14. Herbst RS. Review of epidermal growth factor receptor biology. Int J Radiat Oncol Biol Phys, 2004, 59: 21–26.
15. Huang PH, Xu AM, White FM. Oncogenic EGFR signaling networks in glioma. Sci Signal, 2009, 2: re6.
16. Schlessinger J, Lemmon MA. SH2 and PTB domains in tyrosine kinase signaling. Sci STKE, 2003, 2003: RE12.
17. Azuaje F, Tiemann K, Niclou SP. Therapeutic control and resistance of the EGFR-driven signaling network in glioblastoma. Cell Commun Signal, 2015, 13: 23.
18. Dikic I. Mechanisms controlling EGF receptor endocytosis and degradation. Biochem Soc Trans, 2003, 31: 1178–1181.
19. Ekstrand AJ, Sugawa N, James CD, *et al.* Amplified and rearranged epidermal growth factor receptor genes in human glioblastomas reveal deletions of sequences encoding portions of the N- and/or C-terminal tails. Proc Natl Acad Sci USA, 1992, 89: 4309–4313.
20. Ohgaki H, Dessen P, Jourde B, *et al.* Genetic pathways to glioblastoma: A population based study. Cancer Res, 2004, 64: 6892–6899.
21. Ohgaki H, Kleihues P. Genetic pathways to primary and secondary glioblastoma. Am J Pathol, 2007, 170: 1445–1453.
22. Singh AB, Harris RC. Autocrine, paracrine and juxtacrine signaling by EGFR ligands. Cell Signal, 2005, 17: 1183–1193.
23. Vogt N, Lefevre SH, Apiou F, *et al*. Molecular structure of double-minute chromosomes bearing amplified copies of the epidermal growth factor receptor gene in gliomas. Proc Natl Acad Sci USA, 2004, 101: 11368–11373.
24. Erdem-Eraslan L, Gao Y, Kloosterhof NK, *et al.* Mutation specific functions of EGFR result in a mutation-specific downstream pathway activation. Eur J Cancer, 2015, 51: 893–903.
25. Cancer Genome Atlas Research Network. Comprehensive genomic characterization defines human glioblastoma genes and core pathways. Nature, 2008, 455: 1061–1068.
26. Frederick L, Wang XY, Eley G, *et al*. Diversity and frequency of epidermal growth factor receptor mutations in human glioblastomas. Cancer Res, 2000, 60: 1383–1387.
27. Lee JC, Vivanco I, Beroukhim R, *et al.* Epidermal growth factor receptor activation in glioblastoma through novel missense mutations in the extracellular domain. PLoS Med, 2006, 3: e485.
28. Zandi R, Larsen AB, Andersen P, *et al*. Mechanisms for oncogenic activation of the epidermal growth factor receptor. Cell Signal, 2007, 19: 2013–2023.
29. Humphrey PA, Gangarosa LM, Wong AJ, *et al.* Deletion-mutant epidermal growth factor receptor in human gliomas: effects of type II mutation on receptor function. Biochem Biophys Res Commun, 1991, 178: 1413–1420.
30. Wong AJ, Ruppert JM, Bigner SH, *et al*. Structural alterations of the epidermal growth factor receptor gene in human gliomas. Proc Natl Acad Sci USA, 1992, 89: 2965–2969.
31. Garcia de Palazzo IE, Adams GP, Sundareshan P, *et al*. Expression of mutated epidermal growth factor receptor by non-small cell lung carcinomas. Cancer Res, 1993, 53: 3217–3220.
32. Moscatello DK, Holgado-Madruga M, Godwin AK, *et al*. Frequent expression of a mutant epidermal growth factor receptor in multiple human tumors. Cancer Res, 1995, 55: 5536–5539.
33. Mosesson Y, Mills GB, Yarden Y, *et al.* Derailed endocytosis: an emerging feature of cancer. Nat Rev Cancer, 2008, 8: 835–850.
34. Huang PH, Mukasa A, Bonavia R, *et al.* Quantitative analysis of EGFRvIII cellular signaling networks reveals a combinatorial therapeutic strategy for glioblastoma. Proc Natl Acad Sci USA, 2007, 104: 12867–12872.
35. Schulze WX, Deng L, Mann M. Phosphotyrosine interactome of the ErbB-receptor kinase family. Mol Syst Biol, 2005, 1: 2005.0008.

36. Aaronson DS, Horvath CM. A road map for those who don't know JAK-STAT. Science, 2002, 296: 1653–1655.
37. Levy DE, Lee CK. What does STAT3 do? J Clin Invest, 2002, 109: 1143–1148.
38. de la Iglesia N, Konopka G, Puram SV, *et al*. Identification of a PTEN-regulated STAT3 brain tumor suppressor pathway. Genes Dev, 2008, 22: 449–462.
39. Sun Y, Zhang W, Chen D, *et al*. A glioma classification scheme based on coexpression modules of EGFR and PDGFRA. Proc Natl Acad Sci USA, 2014, 111: 3538–3543.
40. Carvalho PO, Uno M, Oba-Shinjo SM, *et al*. Activation of EGFR signaling from pilocytic astrocytomas to glioblastomas. Int J Biol Markers, 2014, 29: e120–128.
41. Pedeutour-Braccini Z, Burel-Vandenbos F, Gozé C, *et al*. Microfoci of malignant progression in diffuse low-grade gliomas: towards the creation of an intermediate grade in glioma classification? Virchows Arch, 2015, 466: 433–444.
42. Katanasaka Y, Kodera Y, Kitamura Y, *et al*. Epidermal growth factor receptor variant type III markedly accelerates angiogenesis and tumor growth via inducing c-myc mediated angiopoietin-like 4 expression in malignant glioma. Mol Cancer, 2013, 12: 31.
43. Cimino PJ, Bredemeyer A, Abel HJ, *et al*. A wide spectrum of EGFR mutations in glioblastoma is detected by a single clinical oncology targeted next-generation sequencing panel. Exp Mol Pathol, 2015, 98: 568–573.

DOI 10.1007/s10330-016-0135-y
Cite this article as: Ke CS. Epidermal growth factor receptor: a key manipulator in molecular pathways of malignant glioma. Oncol Transl Med, 2016, 2: 99–103.

Oncology and Translational Medicine
DOI 10.1007/s10330-015-0126-4

June 2016, Vol. 2, No. 3, P104–P109

ORIGINAL ARTICLE

Non-specific histological variant of dysembryoplastic neuroepithelial tumor: a diagnostic challenge

Yanyang Chen[1], Bin Li[1], Boning Luo[2], Xiaoying Tian[3], Zhi Li[1] (✉)

[1] Department of Pathology, The First Affiliated Hospital, Sun Yat-sen University, Guangzhou 510080, China
[2] Department of Radiology, The First Affiliated Hospital, Sun Yat-sen University, Guangzhou 510080, China
[3] School of Chinese Medicine, Hong Kong Baptist University, Hong Kong, China

Abstract

Objective The accurate diagnosis of the non-specific variant of dysembryoplastic neuroepithelial tumor (DNT) is very difficult because it is characterized by absence of the histological hallmark of the "specific glioneuronal element" in lesions. We herein present two cases of the non-specific form of DNT to analyze the clinical, radiological, and histological features of this unusual subtype of DNT.

Methods A 16-year-old and a 23-year-old patient had been treated for pharmacoresistant epilepsy for several years before undergoing referral to the hospital for further examination and treatment. Magnetic resonance imaging (MRI) revealed that both patients had a small, well-demarcated cystic lesion within the cortex of the brain without obvious contrast enhancement or peritumoral edema. The lesions were totally resected and routinely examined using histological and immunohistochemical analysis.

Results Both lesions exhibited similar histological appearances with cyst formation and mural nodule architecture. The glial nodules were mainly composed of oligodendrocyte-like components, and partly of piloid cells resembling pilocytic astrocytoma. The cortex adjacent to the lesion in both cases was found to have the histological features of focal cortical dysplasia (FCD) Type I. Immunohistochemically, the oligodendrocyte-like components were diffusely positive for Syn and Olig-2, but staining for CD34, p53, and IDH1 R132H was negative. The Ki-67 (MIB-1) labeling index was low, approximately 1%. There was no 1p/19q co-deletion in either lesion by fluorescence in situ hybridization (FISH) assay. Neither patient received postoperative adjuvant treatment, and both underwent regular follow-up for at least 24 months. No signs of recurrence or epileptic attacks were observed during the follow-up period.

Conclusion The non-specific variant of DNT is a diagnostic challenge for pathologists in clinical practice, and differentiation from some low-grade gliomas needs to be considered. The careful inspection of radiologic and histopathologic findings, accompanied by analysis of patients' clinical manifestations, may be helpful in making an accurate diagnosis.

Received: 16 December 2015
Revised: 13 January 2016
Accepted: 25 March 2016

Keywords: brain tumor; dysembryoplastic neuroepithelial tumor; cortical dysplasia; differential diagnosis

Dysembryoplastic neuroepithelial tumor (DNT) is a benign tumor entity that is usually located in the supratentorial cortex and frequently occurs in children or young adults. According to the World Health Organization (WHO) classification in 1993, 2000, and 2007, DNTs belong to the category of "neuronal and mixed neuronal-glial tumors", are characterized by drug-resistant partial seizures, and are often associated with cortical dysplasia [1]. Histologically, three morphological variants have been described, namely, simple, complex, and non-specific forms. The histological hallmark of the DNTs is the "specific glioneuronal element", in which bundles of axons lined by small oligodendroglia-like cells (OLCs) and large floating neurons within mucinous pools may be typically observed in simple and complex variants. Glial nodules, which lend the tumor a characteristic multinodular architecture, are also seen in complex forms with the specific glioneuronal element [2]. However, the concept of non-specific variants of DNT, which were firstly described by Daumas-Duport in 1999, remains controversial, as these

✉ Correspondence to: Zhi Li. Email: lizhi@mail.sysu.edu.cn

variants lack the specific glioneuronal element and multinodular architecture [3]. In clinical practice, non-specific variants of DNTs often present a diagnostic challenge and may be confused with low-grade gliomas. However, the accurate diagnosis of DNTs is important because patients with DNTs misdiagnosed as gliomas will receive adjuvant radiation and/or chemotherapy inappropriately. We herein report two cases of the non-specific variant of DNT in young patients. The clinical and histological features of this rare histological form, as well as differential diagnosis, are discussed.

Materials and methods

Patients and clinical manifestations

Case 1. A 16-year-old boy presented with a history of at least two complex seizures over the previous three years. According to his parents, he had been treated unsuccessfully with antiepileptic drugs. As a result, the patient was referred to our hospital for further examination and treatment. Magnetic resonance imaging (MRI) revealed a small, well-demarcated cystic lesion within the cortex of the left frontal lobe that was 1.0 × 1.0 × 1.0 cm in size, and a mural nodule could be observed on the cystic wall. The lesion appeared hypointense on T1-weighted images and hyperintense on T2-weighted images. Contrast-enhanced imaging displayed mild heterogeneous enhancement of the lesion. There was no obvious peritumoral edema or mass effect (Fig. 1). A subdural grid recording revealed that the epileptic focus lay in the cortex covering the lesion. The clinical diagnosis was epilepsy-related low-grade glioma or ganglioglioma. The lesion was completely removed surgically. The mass appeared grayish and was covered with normal-looking cortex. No postoperative radiotherapy or chemotherapy was administered. After surgery, the patient underwent regular follow-up for 24 months, and there was no evidence of recurrence in that period.

Case 2. A 23-year-old female patient presented with progressive headache, nausea, and vomiting for five months. She had been diagnosed with focal epilepsy with seizure onset at the age of 10, but no abnormal findings were present in general or on neurological examination. MRI scans revealed a large non-enhanced cystic lesion with a mural nodule, measuring 5.5 × 3.0 × 1.0 cm, in the cortex of the left temporal lobe. The lesion appeared hypointense on T1-weighted images and hyperintense on T2-weighted images, with mild peritumoral edema, but no contrast enhancement was observed (Fig. 2). The lesion was removed via a standard left craniotomy. At surgery, the lesion was observed to be poorly vascularized and the border between the lesion and the normal brain was demarcated. Total resection was achieved. The postoperative course was uneventful and no postoperative radiotherapy or chemotherapy was administered. The patient underwent follow-up for 36 months without any evidence of tumor recurrence. No further epileptic attacks were observed during the follow-up period.

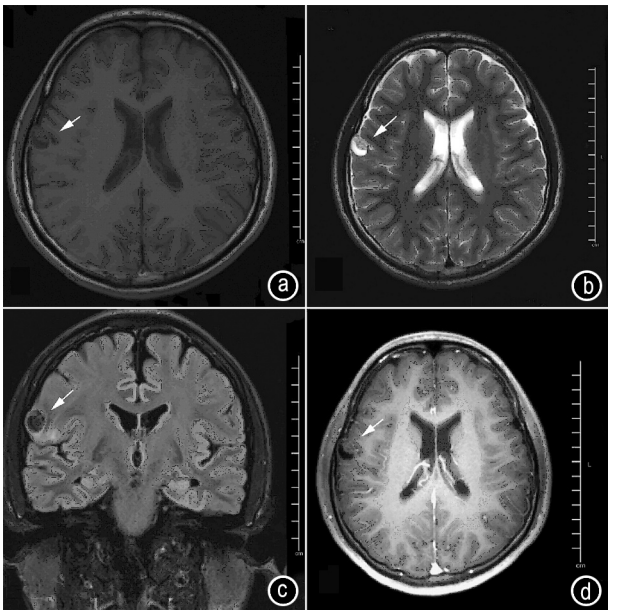

Fig. 1 Pre-operative MRI of the lesion of Case 1. (a) T1-weighted axial MRI demonstrated a hypointense lesion in the left frontal lobe containing a circumscribed cystic component and solid mural nodule (white arrow); (b) T2-weighted axial MRI showed a well-circumscribed lesion was located in the cortex of brain with high intensity of fluid content of the cyst and low intensity of a solid component without obvious peri-tumoral edema (white arrow); (c) On coronal MRI, the lesion was observed to be located in the cortex completely (white arrow), and (d) there was no remarkable contrast enhancement after administration of Gd-DTPA (white arrow)

Pathological examination

Both surgical specimens were fixed with 10% buffered formalin and embedded in paraffin for histological examination. Four-μm-thick sections were stained with hematoxylin and eosin (H&E). Immunohistochemical staining of paraffin sections was performed using the ChemMate Envision/HRP Kit (Dako, Glostrup, Denmark). The primary antibodies used in this study were: GFAP, vimentin, pan-cytokeratin (AE1/AE3), S-100 protein, oligodendrocyte transcription factor 2 (Olig-2), neuronal nuclei (NeuN), synaptophysin (Syn), CD34, IDH1 R132H, p53, and Ki-67.

For cytogenetic analysis, 1p/19q co-deletion in both lesions was detected by fluorescence in situ hybridization (FISH) utilizing the Vysis Dual Color Break Apart Probe (Vysis, Abbott Laboratories Inc., Maidenhead, UK). We detected 1p36 and 19q13 as target probes and 1q25 and 19p13 as control probes in paraffin-embedded sections in accordance with the manufacturer's protocol.

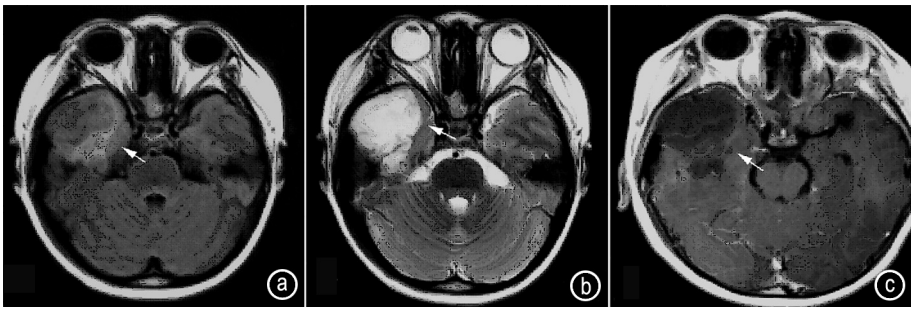

Fig. 2 Pre-operative MRI of the lesion of Case 2. (a) T1-weighted axial MRI exhibited a large hypointense cystic lesion with a mural nodule in the cortex of left temporal lobe (white arrow); (b) But the lesion was hyperintense on T2WI, with mild peri-tumoral edema (white arrow); (c) There was no contrast enhancement was observed in lesion (white arrow)

Results

Histopathological findings

On microscopic examination, both lesions exhibited similar histological appearances. The well-demarcated lesions were located within the cortex and partly extended into the adjacent cortex. They were non-encapsulated and displayed a cystic formation. No specific glioneuronal element with floating neurons within small mucoid lakes was found in either lesion. However, glial nodules, which constituted mural nodules on the cyst walls in both cases, were seen in association with the cystic architecture. The glial nodules were mainly composed of oligodendrocyte-like components, which showed a monomorphic appearance with uniform round nuclei and perinuclear halos. Scattered neuronal cells were observed to be embedded in the oligodendrocyte-like components. However, in contrast to typical oligodendrogliomas, no branching network of capillaries was present (Fig. 3a–c). In some areas of glial nodules, piloid cells with long, hair-like processes, resembling pilocytic astrocytoma, were identified (Fig. 3d). However, there were no Rosenthal fibers or eosinophilic granular bodies in either lesion. In addition, the cortex adjacent to the lesion in both cases was found to have the histological features of focal cortical dysplasia (FCD) Type I. In those areas, blurring of layer boundaries and distinct microcolumnar arrangements, which were composed of more than eight small diameter neurons, could be identified by NeuN immunohistochemistry (Fig. 3e–f, Fig. 4e).

Immunohistochemical and FISH findings

Immunohistochemically, the oligodendrocyte-like component was diffusely positive for Syn and Olig-2 and focally positive for S-100 protein. The scattered neuronal cells were positive for NeuN. The piloid cells in the lesions were positive for GFAP and Olig-2. However, there was no positive signal found for detection of pan-cytokeratin, CD34, P53, or IDH1 R132H. The Ki-67 (MIB-1) labeling index was only 1% focally (Fig. 4a–d). A total of 200 cells were observed for chromosomal abnormalities. We utilized 1p36 and 19q13 as target probes and 1q25 and 19p13 as control probes. Based on a cutoff value of 20%, there was no 1p/19q co-deletion found in either case (Fig. 4f).

On the basis of clinical manifestations, radiological features, and histopathological appearance; cortical location; cystic and mural nodule architecture without specific glioneuronal element; and the presence of FCD in adjacent cortex, a pathological diagnosis of DNT, non-specific variant, WHO grade I, was made.

Discussion

DNTs were first characterized by Daumas-Duport and his colleagues in 1988 to describe a surgically curable tumor found in young patients with intractable partial seizures [4]. Since 1993, the WHO classification of tumors of the central nervous system has accepted DNTs as a unique entity of "neuronal and mixed neuronal-glial tumors" [1]. However, at that time, the histological criteria of DNT were based on the initial description by Daumas-Duport and allowed only for the diagnosis of a morphological variant now referred to as the "complex form". In 2000 and 2007, the "simple form" and "non-specific form" of DNT were additionally described as unique variants of DNTs in later editions of the WHO classification [1, 5].

It has been suggested that DNTs include a large spectrum of tumors that cannot be distinguished histologically from ordinary gliomas, and that the diagnosis of such "non-specific histological forms" requires that clinical presentation and imaging features be taken into consideration. Because the "non-specific form" of DNTs lacks the specific glioneuronal element and multinodular architecture, this variant of DNTs is often histologically indistinguishable from low-grade gliomas, particularly when the cortical topography of the tumor is not apparent on non-representative samples. Therefore, it is important for neuropathologists that the diagnosis of DNT be considered whenever all of the following criteria are present: (I) partial seizures with or without secondary generalization, usually beginning before the age of 20 years; (II) no progressive neurological deficit; (III) predominantly cortical topography of a supratentorial lesion, best demonstrated on MRI; and (IV) no mass effect on computed tomography (CT) or MRI, except if related to a cyst, and no peritumor-

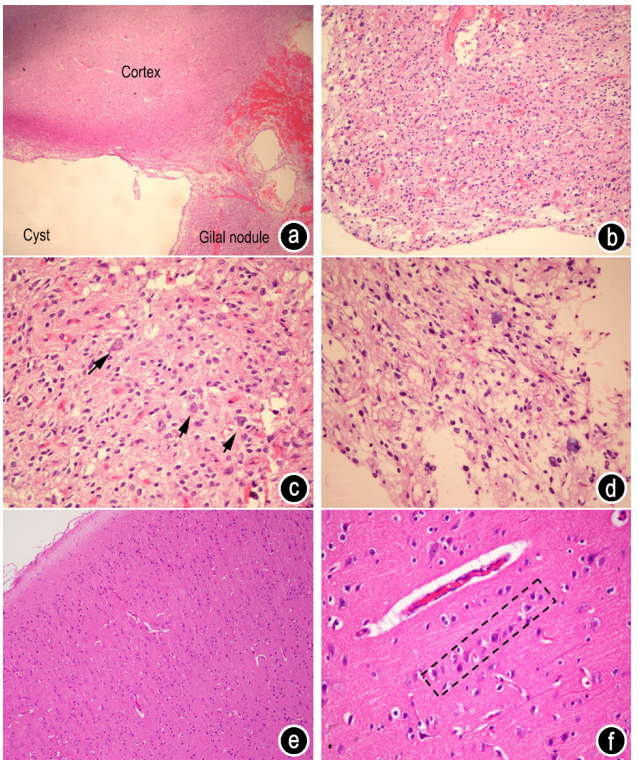

Fig. 3 Histological features of lesions in both cases. (a) At the lower power fields, the lesions could be found to be composed of cyst, cortex and glial nodule; (b) The glial nodule was mainly composed of oligodendrocytic-like cells with uniform round nuclei and perinuclear halos, resembling oligodendroglioma; (c) Scattered neuronal cells (black arrows) were observed to be embedded in the oligodendrocytic-like components; (d) In the some areas of glial nodules, piloid cells with long, hair-like processes, resembling pilocytic astrocytoma were identified, but there were no Rosenthal fibers and eosinophilic granular bodies in lesions; (e) The adjacent cortex of lesions was found to have the histological features of focal cortical dysplasia (FCD) Type I with blurring of layer boundaries and distinct microcolumnar arrangements; (f) At the higher power fields, a microcolumnar arrangement, which were composed of more than eight small diameter neurons could be identified (black dashed box) (a and e, HE staining × 100; b–d, f, HE staining × 400)

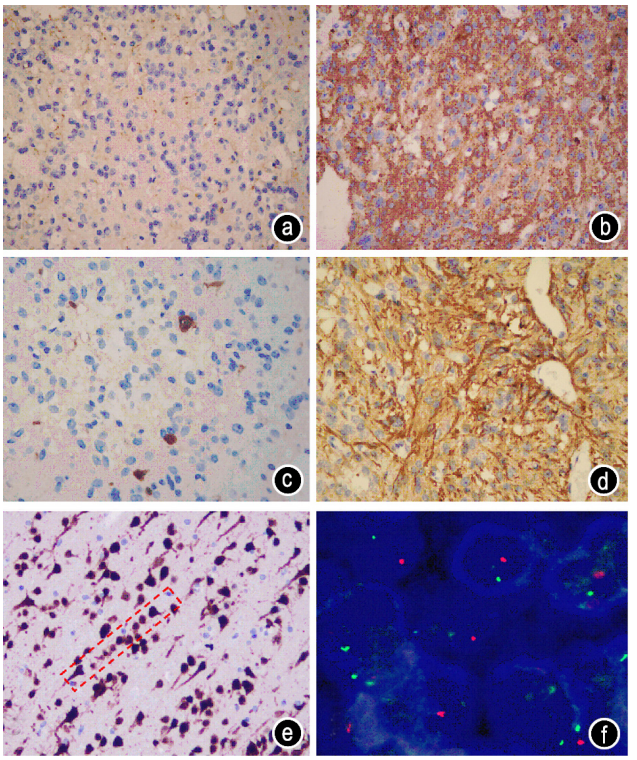

Fig. 4 Immunohistochemical and FISH assay of lesions. (a) The oligodendrocytic-like cells in glial nodule were negative for GFAP, but were diffusely positive for Syn (b); (c) The scattered neuronal cells were observed to have positive signal to Neu N; (d) However, the piloid cells with long, hair-like processes showed GFAP immuno-positivity; (e) NeuN immunohistochemical staining exhibited the microcolumnar arrangement in adjacent cortex with FCD (red dashed box); (f) FISH assay showed that there was no 1p/19q co-deletion in both lesions. The figure only showed FISH assay for 1p, the data of 19q detection was not shown here (a–e, immunohistochemical staining with original magnification × 400; f, FISH assay × 400)

al edema [1, 3]. In our cases, both patients had a supratentorial intracortical lesion with cyst formation, and no peritumoral edema or contrast enhancement was observed . They were young patients without neurological deficits or mass effect on MRI examination. The entire clinical presentation and all radiological features were consistent with the diagnostic criteria for DNTs. Furthermore, as in the complex form of DNTs, foci of cortical dysplasia could be identified in the cortex adjacent to both lesions. Such dysplastic changes in our cases strongly suggested that these tumors belonged to the category of DNTs.

Due to the absence of the specific glioneuronal element, which is characterized by parallel strands of axons, oligodendrocyte-like cells, and floating ganglion cells in microcystic mucopolysaccharide-rich areas [1], the diagnoses in our cases remain controversial. In addition, the histological appearance of oligodendroglioma-like and pilocytic astrocytoma-like areas in the lesions engenders diagnostic confusion with other low-grade infiltrating neoplasms, such as ganglioglioma, oligodendroglioma, and central neurocytoma. It has been documented that DNT has areas composed of astrocytic, oligodendroglial, and neuronal components. Theoretically, overgrowth of any of these may result in an independent tumor [1–4]. However, gangliogliomas, the presence of abnormal neurons, and lymphocytic cuffing were not observed in our cases. It is now well known that oligodendrogliomas are often characterized by 1p/19q co-deletion and mutation in the IDH1 gene [6–7]. In the present tumors, 1p/19q co-deletion and expression of mutant IDH1 were not detectable. The combination of these two negative findings is suggestive of DNT rather than oligodendroglioma. It is important to note that the precise origin of the OLCs in DNTs is still

unknown. Some of these cells express neuronal markers and exhibit synaptophysin, suggesting that the OLCs of DNTs may show an early neuronal differentiation [8–9]. However, recent results with in situ hybridization demonstrated that OLCs transcribe myelin genes and express myelin oligodendrocyte glycoprotein protein, indicating oligodendroglial differentiation [10]. Results from some studies have suggested that DNTs are originally oligodendrogliomas that occur preferentially in the cerebral cortex and have more benign biological behavior, corresponding to WHO grade I [11].

Although DNTs have been subcategorized into simple, complex or non-specific histological forms, we are well aware of the fact that there have been no clinical or therapeutic implications related to the different histological forms. Different histological subtypes of DNT might only reflect varied histological features and remind pathologists to avoid over-diagnosing lesions as low-grade or even high-grade gliomas or gangliogliomas. As there is no specific immunohistochemical marker for recognition of different subtypes of DNTs, we herein emphasize that the diagnosis of DNTs should be confirmed by clinical, radiological, and histological characteristics of patients. If there is absence of the specific morphological features in the lesion, all of the four criteria described above must be present to make an accurate diagnosis. In our experience, the diagnosis of the non-specific form of DNT should be considered particularly in children or young patients in cases in which a glial tumor exhibits an unusual histological appearance without the specific glioneuronal element, but showing a supratentorial intracortical lesion without peritumoral edema and mass effect. If the case presents diagnostic difficulties, close surveillance by imaging might be a better plan to objectively determine the actual behavior of the tumor, because radiotherapy and chemotherapy are contraindicated for DNTs [12–14]. Previously reported DNTs have usually shown no evidence of recurrence following resection. However, some studies have suggested that tumor recurrence after gross total resection or enlargement of the residual tumor with subtotal resection of DNTs may occur. There have even been reports that have documented tumor progression [15–16] or malignant transformation [17–18]. Risk factors for the development of recurrent seizures after operation on long-term follow-up included longer preoperative history of seizures, presence of residual tumor, and presence of cortical dysplasia adjacent to DNT [19–21]. Therefore, we suggest that a long period of follow-up is necessary even if the patient experienced complete relief upon initial surgical treatment.

In conclusion, we report two additional rare cases of the non-specific form of DNT with favorable prognosis occurring in young patients. Both tumors exhibited the conventional clinical manifestations and radiological appearance of DNTs, but lacked the specific histological features. In clinical practice, non-specific variants of DNTs are a diagnostic challenge for pathologists and may be confused with other low-grade gliomas. The careful inspection of radiologic and histopathologic findings may be helpful to make an accurate diagnosis.

References

1. Louis DN, Ohgaki H, Wiestler OD, *et al*. WHO classification of tumours of the central nervous system. Lyon: IARC Press. 2007.
2. Daumas-Duport C. Dysembryoplastic neuroepithelial tumours. Brain Pathol, 1993, 3: 283–295.
3. Daumas-Duport C, Varlet P, Bacha S, *et al*. Dysembryoplastic neuroepithelial tumors: nonspecific histological forms-a study of 40 cases. J Neurooncol, 1999, 41: 267–280.
4. Daumas-Duport C, Scheithauer BW, Chodkiewicz JP, *et al*. Dysembryoplastic neuroepithelial tumor: a surgically curable tumor of young patients with intractable partial seizures. Report of thirty-nine cases. Neurosurgery, 1988, 23: 545–556.
5. Kleihues P, Cavenee WK. WHO classification of tumors of the nervous system. Lyon: IARC Press. 2000.
6. Reifenberger G, Kros JM, Louis DN, *et al*. Oligodendroglioma. In: Louis DN, Ohgaki H, Wiestler OD, *et al*. WHO classification of tumors of the central nervous system, 4th edn. Lyon: IARC Press, 2007. 54–59.
7. Thom M, Blümcke I, Aronica E. Long-term epilepsy associated tumors. Brain Pathol, 2012, 22: 359–379.
8. Wolf HK, Buslei R, Blumcke I, *et al*. Neural antigens in oligodendrogliomas and dysembryoplastic neuroepithelial tumors. Acta Neuropathol, 1997, 94: 436–443.
9. Hirose T, Scheithauer BW, Lopes MB, *et al*. Dysembryoplastic neuroeptihelial tumor (DNT): an immunohistochemical and ultrastructural study. J Neuropathol Exp Neurol, 1994, 53: 184–195.
10. Gyure KA, Sandberg GD, Prayson RA, *et al*. Dysembryoplastic neuroepithelial tumor: an immunohistochemical study with myelin oligodendrocyte glycoprotein. Arch Pathol Lab Med, 2000, 124: 123–126.
11. Takahashi H, Kakita A, Tomikawa M, *et al*. Oligodendroglioma (WHO grade I) in a young epilepsy patient: a specific entity lying within the spectrum of dysembryoplastic neuroepithelial tumor? Neuropathology, 2013, 33: 645–651.
12. Taratuto AL, Pomata H, Sevlever G, *et al*. Dysembryoplastic neuroepithelial tumor: morphological, immunocytochemical and deoxyribonucleic acid analyses in a pediatric series. Neurosurgery, 1995, 36: 474–481.
13. Raymond AA, Fish DR, Sisodiya SM, *et al*. Abnormalities of gyration, heterotopias, tuberous sclerosis, focal cortical dysplasia, microdysgenesis, dysembryoplastic neuroepithelial tumour and dysgenesis of the archicortex in epilepsy. Clinical, EEG and neuroimaging features in 100 adult patients. Brain, 1995, 118: 629–660.
14. Ranger A, Diosy D. Seizures in children with dysembryoplastic neuroepithelial tumors of the brain-A review of surgical outcomes across several studies. Childs Nerv Syst, 2015, 31: 847–855.
15. Sampetrean O, MaeharaT, Arai N, *et al.* Rapidly growing dysembryoplastic neuroepithelial tumor: case report. Neurosurgery, 2006, 59: E1337–1338.
16. Daghistani R, Miller E, Kulkarni AV, *et al*. Atypical characteristics and behavior of dysembryoplastic neuroepithelial tumors. Neuroradiology, 2013, 55: 217–224.

17. Hammond RR, Duggal N, Woulfe JM. Malignant transformation of a dysembryoplastic neuroepithelial tumor. Case report. J Neurosurg, 2000, 92: 722–725.
18. Chae JH, Kim SK, Wang KC. Hemifacial seizure of cerebellar ganglioglioma origin: seizure control by tumor resection. Epilepsia, 2001, 42: 1204–1207.
19. Aronica E, Leenstra S, van Veelen CW, *et al.* Glioneuronal tumors and medically intractable epilepsy: a clinical study with long-term follow-up of seizure outcome after surgery. Epilepsy Res, 2001, 43: 179–191.
20. Sakuta R, Otsubo H, Nolan MA, *et al.* Recurrent intractable seizures in children with cortical dysplasia adjacent to dysembryoplastic neuroepithelial tumor. J Child Neurol, 2005, 20: 377–384.
21. Nolan MA, Sakuta R, Chuang N, *et al*. Dysembryoplastic neuroepithelial tumors in childhood: long-term outcome and prognostic features. Neurology, 2004, 62: 2270–2276.

DOI 10.1007/s10330-015-0126-9
Cite this article as: Chen YY, Li B, Luo BN, *et al*. Non-specific histological variant of dysembryoplastic neuroepithelial tumor: a diagnostic challenge. Oncol Transl Med, 2016, 2: 104–109.

Oncology and Translational Medicine
DOI 10.1007/s10330-016-0132-1

June 2016, Vol. 2, No. 3, P110–P114

CASE REPORT

Fibroblastic reticular cell sarcoma of the small intestine: a very rare case report and clinicopathological diagnosis

Dingrong Zhong[1], Dong Wu[2] (✉)

[1] Department of Pathology, Peking Union Medical College Hospital, Peking Union Medical College and Chinese Academy of Medical Sciences, Beijing 100730, China
[2] Department of Gastroenterology, Peking Union Medical College Hospital, Peking Union Medical College and Chinese Academy of Medical Science, Beijing 100730, China

Abstract

A 54-year-old man was admitted for the evaluation of fever and abodominal pain. Radiological and endoscopic examination revealed a lung nodule and multiple small intestine uclers. Clinical diagnosis such as tuberculosis and Crohn's disease had been proposed. He developed intestine perforation after small bowel endoscopic procedure. During emergent surgery the involved intestinal segments were resected and a pathological diagnosis of fibroblastic histiocytic sarcoma (FBRC) was made. The patient died in the sixth month after the operation. The management of this cases highlighted the drawback of pattern recognition as the most commonly used clinical reasoning method, and the importance of histological investigation.

Received: 18 January 2016
Revised: 25 February 2016
Accepted: 25 March 2016

Key words: fibroblastic histiocytic sarcoma; tuberculosis; Crohn's disease; small bowel endoscopy; pattern recognition

A 54-year-old man was referred to our hospital because of abdominal pain and fever. According to the principle of Occam's Razor, we needed to find an inflammatory or neoplastic etiology to explain both symptoms. The patient had been healthy until 3 months before admission. He had intermittent colic around the umbilicus with exacerbation after eating. The patient rated his pain 6–10 on a 10-point scale. The pain did not radiate, was not related to position, and did not improve with the use of a proton-pump inhibitor. A low-grade fever occurred 4 weeks prior to admission. He had night sweats and a 15-kg weight loss. He did not experience cough, chills, melena, hematochezia, vomiting, dysphagia, or altered bowel habits. Pulmonary tuberculosis was diagnosed in the patient 25 years before and resolved after therapy. He had a 45-year history of smoking a pack of cigarettes a day and on average consumed 50 g of alcohol per day for the last 20 years.

On examination, the patient looked chronically ill and cachectic but alert and oriented. His temperature was 38.0°C, his heart rate was 92 beats per min, his respiratory rate was 18 breaths per min, his blood pressure was 106/70 mmHg, and his oxygen saturation was 95 percent while he was breathing ambient air. His weight was 48 kg, and his height was 1.72 m. No lymphadenopathy, icterus, spider angioma, or liver palm was present. The oropharynx was clear. The patient's neck was supple without bruits or goiter. Cardiac examination was normal. His lungs were normal except for decreased breath sounds from both sides. The abdomen was scaphoid without subcutaneous varicose veins. Bowel sounds were normal, and shift dullness was negative. On palpation, the abdomen was soft with tenderness in the left upper and right lower quadrant. No rebound, rigidity, or organomegaly was revealed. Rectal examination revealed no mass. A stool sample was positive for occult blood. He had no peripheral edema. His neurological examination was normal.

Laboratory studies revealed a white cell count of 9200 per cubic millimeter, with 67 percent neutrophils, a platelet count of 337,000 per cubic millimeter, and a hematocrit of 30 percent, with a mean corpuscular volume of 79 μm3. Electrolytes, liver function tests, amylase,

✉ Correspondence to: Dong Wu. Email: wudong061002@aliyun.com

and coagulation were normal, except for a serum albumin concentration of 3.2 g per deciliter. Urinalysis was normal. His erythrocyte sedimentation rate was 103 mm per hour. Tests of blood cultures, interferon gamma release assay, serum deoxyribonucleic acid for cytomegalovirus, antinuclear antibody, and anti-neutrophil cytoplasm antibody were all negative. A chest radiograph was consistent with chronic obstructive lung disease and resolved tuberculosis.

A gastroduodenoscopy and a colonoscopy with terminal ileal intubation were performed, but they did not reveal any remarkable abnormalities. An air-barium double contrast examination of the small bowel showed multiple ulcers in the jejunum and ileum between normal mucosa (Fig. 1a). Computed tomography (CT) enterography showed skip lesions in the small intestine, including segmental thickening of the bowel wall, marked mucosal enhancement, and lymphadenopathy (Fig. 1b). A CT scan of the lungs incidentally identified a 3.0 × 2.2 cm nodule in the left lower lung with a vessel within it, as well as resolved tuberculosis (Fig. 1c and 1d). Capsule endoscopy was ordered and illustrated large ulcers in the jejunum and ileum with normal mucosa between two lesions (Fig. 1e).

The lung CT findings were not very clear. The location of the nodule explains why it was overlooked on radiograph. The smooth margin of the nodule and the lack of satellite lesions were incompatible with pulmonary tuberculosis. Given the patient's age, the size of the nodule, and the history of heavy smoking, lung cancer should never be excluded. The diffuse involvement of the small bowel, however, cannot be readily explained by lung cancer, because gastrointestinal metastasis of lung cancer is rare. According to a series of case reports, gastrointestinal metastasis usually occurs in the end stages of widely metastatic disease and typically presents with bowel obstruction, massive hemorrhage, and perforation. Although normal ileocecum is infrequent in Crohn's disease, it was a strong differential diagnosis, particularly considering the skip lesions in the small bowel. Among the extra-intestinal manifestations of Crohn's disease, lung involvement is uncommon. However, literature of such manifestations is accumulating and includes drug-related pathologies, airway disease, fistulas, granulomatous disorders, and autoimmune and thromboembolic events. Therefore, the nodule could have theoretically developed in the background of established Crohn's disease.

A pulmonologist saw the patient and agreed that the nodule was inconsistent with tuberculosis. However, he could not relate the pulmonary findings to the small bowel abnormality. The results of microbiological investigations of an induced sputum sample were negative, including Gram stain and acid-fast staining and culture. A bronchoscopy was performed, and the bronchus was patent. A blind biopsy was obtained and revealed unspecific inflammation. The interventionist declined to perform a needle aspiration of the nodule given the risk of hemorrhage. Surgical resection was also considered risky in light of the patient's impaired lung function and poor general status. Double-balloon enteroscopy revealed a large and deep ulcer in the upper jejunum (Fig. 1f). A biopsy was taken. On the next day, the patient complained of abdominal distention, and plain radiography confirmed free subphrenic air. The patient was diagnosed with perforation, and an exploratory laparotomy was performed.

Small intestinal perforation after small bowel enteroscopy is a serious complication in this case, but it was unsurprising. The risk of such an event was relatively high due to the large and deep ulcers in the small intestine. On the other hand, emergency laparotomy undoubtedly put the patient at risk for post-operation complications, but it also provided case management information since surgical resection of the small intestine would lead to a definite histological diagnosis.

During the operation, three ulcerous tumors in the jejunum and ileum were found. The most proximal tumor was perforated, and the other two nearly perforated. Segmental small bowel resections were performed, and a total of 90 cm of the small intestine was removed. The post-operation recovery was complicated by surgical wound infection, but the patient was administered antibiotics and supportive care and did well after all. A pathologist made the final diagnosis of fibroblastic histiocytic sarcoma (FBRC). The patient and his family declined chemotherapy and chose traditional Chinese medicine instead. On follow-up, he developed hemoptysis, fever, and an abdominal mass in the fourth month after discharge and died two months later.

The pathological examination was described hereafter. About 90 cm of the small intestine was sent to the pathology department for gross examination, and three tumors involving all layers of the intestine with ulcers were found (Fig. 1g), the largest one of which was perforated. Some swollen lymph nodes were found adjacent to the tumors. Histologically, the tumor cells originated from submucosal tissue and heavily infiltrated surrounding tissue (Fig. 1h). Tumor cells infiltrated into the mucous membrane to form an ulcer and invaded into the serosa with local perforation. The tumor cells were spindle-shaped and oval with prominent nucleoli and many mitotic figures without obvious nuclear anaplasia. Extensive tumor necrosis and mild lymphocyte infiltration among tumor cells were observed (Fig. 1i and 1j). Tumor cells were present in regional lymph nodes (3/16). Immunohistochemically, tumor cells were strongly positive for vimentin (Fig. 1k), CD68 (Fig. 1l), and EGFR (Fig. 1m), There was partial reactivity for AE1/AE3 (Fig. 1n), LCA (leucocyfe common antigen) (Fig. 1o), smooth muscle actin (SMA) (Fig.

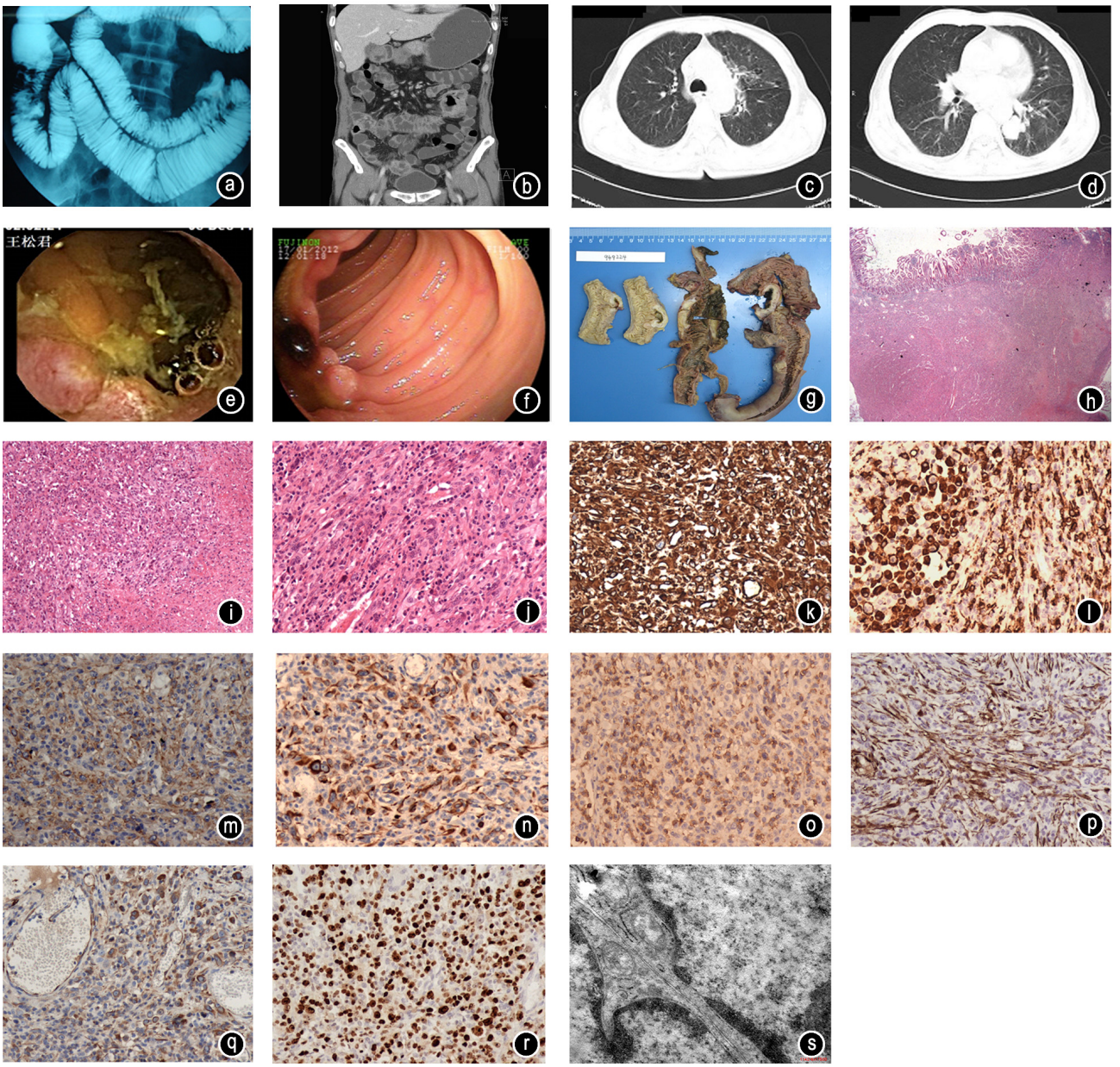

Fig. 1 (a–b) The air-barium and CT enterography showed multiple skip lesions of the small intestine; (c) Old tuberculosis in the left lung; (d) A mass in the left lower lung; (e–f) A large and deep ulcer in the small intestine on capsule endoscopy (e) and small bowel endoscopy (f); (g) Multiple ulcerous tumors in the intestine; (h) The malignancy of submucosal origin and heavy infiltration and invading around tissue (HE staining × 10); (i) Necrosis of the tumor and mild infiltration of lymphocytes (HE staining × 100); (j) Tumor cells with prominent nucleoli and abundant small cytoplasm admixed with lymphocytes (HE staining × 200); (k) Diffuse and strong reactivity for Vimentin (SP × 200); (l) Reactivity for CD68 (SP × 200); (m) Reactivity for EGFR (SP × 200); (n) Partial reactivity for AE1/AE3 (SP × 200); (o) Partial reactivity for LCA (SP × 200); (p) Reactivity for SMA (SP × 200); (q) Reactivity for Desmin (SP × 200); (r) High proportion of Ki-67 expression; (s) Immature desmosomes between tumor cells (electronic microscopy × 17500)

1p), and desmin (Fig. 1q). Tumor cells were negative for CD117, CD34, Dog-1, ALK, CD21, CD35, S100, and CD1a. The Ki-67 tumor index was about 70% (Fig. 1r).

By electron microscope, immature desmosomes were observed (Fig. 1s) between tumor cells; many rough endoplasmic reticulum were present in the cytoplasm of tumor cells.

The pathological diagnosis was FBRC of the small intestine, involving all intestinal layers with metastasis to the regional lymph nodes (3/16).

Discussion

The diagnosis of FBRC relies predominantly on histolytic lineage verification and the exclusion of other poorly

differentiated malignancies by careful histological examination and extensive immunophenotypic investigation [1–5]. Morphologically, FBRC can mimic fibroblasts from other origins with similar long slender cytoplasmic processes, and FBRC can have variable myofibroblastic features [1]. Therefore, definite differentiation between the various entities described above using morphology alone is not possible, and immunohistochemical data plays a key role in these diagnoses [5–7]. In the current classification system of tumors of hematopoietic and lymphoid tissues [8], fibroblastic reticular cell sarcoma has been described as a new subtype, based on the expression of CD68, vimentin, SMA, desmin, and AE1/AE3.

Pathologically, the first disease that merited differentiation in this case was a gastrointestinal stromal tumor (GIST), which is the most common mesenchymal tumor in the alimentary system. GISTs are notorious for their highly variable morphologic features, and they can affect the entire digestive tract with the small intestine as a "hotspot". However, tumor cells in this case were negative for CD117, CD34, and Dog-1, which strongly ruled out diagnosis of this disease. Another possible disease was poorly differentiated carcinosarcoma, and the partial reactivity for AE1/AE3 was suggestive of this possibility, but the origin from the submucosal layer and the positive immunochemical stains with vimentin, SMA, desmin, and CD68 ruled out this malignancy. The immunohistochemical data also helped to exclude other competing diagnoses, such as myofibroblastic tumor, follicular dendritic cell sarcoma, Langerhan's histocytosis, and interdigitating dendritic cell sarcoma. In summary, no malignancy other than FBRC stains positively for SMA, desmin, CD68, and LCA concurrently, as in this case. The electron microscope findings of granular endoplasmic reticulum and underdeveloped desmosomes also support this diagnosis.

Although FBRC tumors are rare, we believe that this case helps to illustrate two important points that apply to general clinical reasoning. First, physicians, especially senior physicians, often employ "pattern recognition" to make a rapid diagnosis. The philosophy of such an approach is that with knowledge and experience, clinicians can form combinations of relevant clinical scenarios (patterns) in their minds that in turn enable each new case to be rapidly evaluated and classified according to its resemblance to existing patterns. To use a metaphor: "If something looks like a duck, walks like a duck, and sounds like a duck, then it is a duck." Although pattern recognition works effectively and efficiently for most problems in daily practice, particularly when quick decision-making is mandatory, such as in an emergency room, it is not immune to cognitive bias and wrong judgments. Furthermore, if physicians anchor to their first impression and refuse adjustment when required, misdiagnosis and errors easily ensue. As for this case, the patient definitely was previously diagnosed with tuberculosis and presented with low fever, night sweats, and weight loss. Therefore, it is quite natural to suspect active abdominal tuberculosis. However, the following diagnostic findings gradually made that diagnosis less likely. On the other hand, when multiple skipping ulcers of the small bowel were found with normal intestinal tissue between them, it was tempting to consider Crohn's disease instead. The nodule in the lungs could also be explained, at least theoretically, by this hypothesis. However, upon thorough consideration, we found many clues that argued against that diagnosis. First, the patient had a rather short clinical course, but he was remarkably wasting. That is not typically seen in Crohn's disease. Secondly, on CT scans, the small intestine was dilated in the first jejunum lesion, while Crohn's disease usually causes strictures of the small intestine. Thirdly, on colonoscopy, the ileocecum, the most common site of Crohn's disease, was normal. To summarize, this case highlights the essential nature of comprehensive evaluation and balanced reasoning of all the relevant data to make good clinical decisions. Even if the clinical scenario seemingly fits a certain diagnosis, rather than jumping to the conclusion, one still needs to arrange necessary diagnostic workups and carefully rule out other competing diagnoses.

The second point of this case is the importance of histological investigation. "Tissue is the issue", and the truth and profundity of this adage can never be overstated. After all other approaches failed to lead to a definite diagnosis, we were left with no choice but to employ enteroscopy to investigate the small intestine. Enteroscopy brought certain risks and resulted in the serious complication of perforation. However, it was perforation that justified emergent laparotomy and led to the eventual pathological diagnosis. Without such an intervention, the patient could have gone undiagnosed for additional time. We also believe that the dramatic course of this case has served to reflect the spirit of Chinese philosophy. According to ancient Chinese thinkers, the natural law governing the universe is a law of cyclic development, and things that develop to one extreme are bound to tend toward the opposite. In other words, nothing is fixed forever. Looking at the perforation from this perspective, we realize that it is a two-fold story. On one hand, perforation is undoubtedly a serious complication and an adverse event, but on the other hand, it also helped to finally diagnose this case. We learned to watch out and take care even in favorable clinical situations and stand resolutely in hard ones. In other words, physicians should withstand adversities in clinical practice, always support their patients, and hope for the best.

Unfortunately, the patient declined post-operative chemotherapy and died shortly thereafter, despite all the

efforts. The natural course of this case was consistent with the highly aggressive behavior of FBRC. Based on his terminal symptoms, we speculated that the pulmonary lesion was probably a metastatic lesion of the disease, and the intra-abdominal tumor had recurred.

Tumors derived from reticular cells are uncommon, and those of FBRC origin are even rarer. Turner et al. described the first well-established case of FBRC in 1984 [2]. In 1998, Andriko *et al* published a report on 11 patients with lymph node reticular cell neoplasms, including 3 cases of FBRC origin [3]. Since then, less than 20 cases of FBRC have been reported that involve lymph nodes, spleen, and liver [4–7, 9, 10]. Although the rarity of FBRC neoplasms has largely prevented a full appreciation of their biological behavior, extranodal presentation is frequent, and the clinical course is generally aggressive in patients with FBRC malignancies. Evidence of FBRC management is scarce. Surgical debulking is the primary treatment option, but the roles of chemotherapy and radiotherapy are unproven. To the best of our knowledge, this is the first case of FBRC sarcoma of the small intestine with a probable lung origin.

Conflicts of interest

The authors indicated no potential conflicts of interest.

References

1. Mueller SN, Germaine RN. Stromal cell contributions to the homeostasis and functionality of the immune system. Nat Rev Immunol, 2009, 9: 618–629.
2. Turner RR, Wood GS, Beckstead JH, *et al*. Histiocytic malignancies: Morphologic, immunologic, and enzymatic heterogeneity. Am J Surg Pathol, 1984, 8: 485–500.
3. Andriko JW, Kaldjian EP, Tsokos M, *et al*. Reticulum cell neoplasms of lymph nodes: a clinicopathologic study of 11 cases with recognition of a new subtype derived from fibroblastic reticular cells. Am J Surg Pathol, 1998, 22: 1048–1058.
4. Chan AC, Serrano-Olmo J, Erlandson RA, *et al*. Cytokeratin-positive malignant tumors with reticulum cell morphology: a subtype of fibroblastic reticulum cell neoplasm. Am J Surg Pathol, 2000, 24: 107–116.
5. Jones D, Amin M, Ordonez NG, *et al*. Reticulum cell sarcoma of lymph node with mixed dendritic and fibroblastic features. Mod Pathol, 2001, 14: 1059–1067.
6. Lucioni M, Bovery E, Rosso R, *et al*. Lymph node reticulum cell neoplasm with progression into cytokeratin-positive interstitial reticulum cell sarcoma: a case study. Histopathology, 2003, 43: 583–591.
7. Martel M, Sarli D, Colecchia M, *et al*. Fibroblastic reticular cell tumor of spleen: report of a case and review of the entity. Hum Pathol, 2003, 34: 954–957.
8. Swerdlow S, Campo E, Harris N. World Health Organization classification of tumors of hematopoietic and lymphoid tissues. Lyon: IARC Press, 2008. 353–367.
9. Schuerfeld K, Lazzi S, De Santi MM, *et al*. Cytokeratin-positive interstitial cell neoplasm: a case report and classification issues. Histopathology, 2003, 43: 491–494.
10. Mücke R, Rechl B, Micke O, *et al*. Surgery and radiotherapy of one rare case with neoplasm derived from fibroblastic reticulum cells of a cervical lymph node. Acta Oncol, 2004, 43: 766–768.
11. Yaman E, Gonul II, Buyukberber S, *et al*. Metastatic fibroblastic reticulum cell sarcoma of the liver: pathologic and PET-CT evaluation. Pathology, 2009, 41: 289–292.

DOI 10.1007/s10330-016-0132-1
Cite this article as: Zhong DR, Dong W. Fibroblastic reticular cell sarcoma of the small intestine: a very rare case report and clinicopathological diagnosis. Oncol Transl Med, 2016, 2: 110–114.

Oncology and Translational Medicine
DOI 10.1007/s10330-016-0148-6

June 2016, Vol. 2, No. 3, P115–P118

ORIGINAL ARTICLE

Bronchoscopic biopsy for diagnosis of lung cancer in the absence of visible endobronchial abnormalities

Hua Zheng[1] (✉), Baohua Lu[1], Qunhui Wang (Co-first author)[1], Fanbin Hu[1], Weimin Ding[2], Baolan Li[1] (✉)

[1] Department of Oncology, Beijing Chest Hospital, Capital Medical University, Beijing 101149, China
[2] Department of Endoscopy, Beijing Chest Hospital, Capital Medical University, Beijing 101149, China

Abstract

Objective Bronchoscopy has been extensively used in the diagnosis of respiratory diseases, and particularly, malignant diseases. However, endoscopists do not normally perform bronchoscopic biopsy in case lesions are undetected via bronchoscopy. The aim of this study was to evaluate whether performing bronchoscopic biopsy could be established in the diagnosis of lung cancer in case of endobronchial abnormalities undetectable to the naked eye.

Methods We retrospectively analyzed 109 cases between January 2008 and December 2012. The inclusion criteria were confirmed lung cancer diagnosis, transbronchial biopsy performed in the absence of visible endobronchial manifestations, brushing, and bronchoalveolar lavage (BAL) according to the images obtained from high-resolution computed tomography (HRCT). Data regarding age, sex, pathology, tumor stage; the method of diagnosis; location of primary lesion (central, peripheral, or intermediate); tumor size, mediastinal lymph node metastasis, and the serum carcinoembryonic antigen (CEA) value were collected. The Pearson chi-square test or Fisher's exact and McNemar tests were used in the univariate analysis.

Results Among the 109 patients, the diagnosis of 37 (33.9%) patients was confirmed through bronchoscopy. Brushing and BAL had higher positive detection rates than biopsy ($P = 0.004$). There were no differences in the positive detection rates between the sex, pathology, lesion location, tumor size, lymph node metastasis, and the serum CEA value ($P > 0.05$ for all groups).

Conclusion Despite the normal appearance of the endobronchial manifestations, lesions undetectable by bronchoscopy could be indicated. Therefore, we suggest performing bronchoscopic biopsy and that brushing and BAL might increase the positive detection rate of bronchoscopic examination.

Received: 1 March 2016
Revised: 12 April 2016
Accepted: 25 April 2016

Key words: bronchoscope; lung cancer; biopsy

Since the application of bronchoscopy [1], the diagnosis of lung disease has become facilitated, which has greatly improved the understanding of respiratory diseases. Bronchoscopy is a critical and indispensable tool, particularly for the diagnosis of pulmonary neoplasms. Because of its safety, convenience, and cost-effectiveness, bronchoscopy has been extensively used in the respiratory department. However, in case of abnormalities undetectable by bronchoscopy, endoscopists do not normally perform bronchoscopic biopsy. This phenomenon might possibly decrease the rate of detection. Furthermore, the lack of a specimen would hinder the identification of genetic mutations that could guide clinical treatment. The aim of this study was to evaluate the role of bronchoscopic biopsy in detecting lung cancer in the presence of lesions undetectable by bronchoscopy.

Materials and methods

Patients

We conducted a retrospective study that included consecutive cases with confirmed diagnoses of lung cancer without visible endobronchial abnormalities, for which a transbronchial lung biopsy (TBLB) was performed depending on the images obtained from high-resolution computed tomography (HRCT) between January 2008

✉ Correspondence to: Baolan Li, Email: libaolan1109@163.com; Hua Zheng, Email: zhenghua022@sina.com

Table 1 Characteristics of the cases

Features	*n*	%
Sex		
Male	64	58.7
Female	45	41.3
Pathology		
Adenocarcinoma	93	85.3
Squamous carcinoma	11	10.1
SCLC	3	2.8
other	2	1.8
Location		
Central	11	10.1
Intermediate	18	16.5
Peripheral	80	73.4

SCLC, small cell lung cancer

Table 2 Positive detection rates of brushing and BAL and biopsy by bronchoscopy

Features	Positive		*P*
	n	%	
Brushing and BAL	34	31.2	0.004
Biopsy	21	19.3	
combined above examinations	37	33.9	

and December 2012. In total, 109 patients were enrolled. The variables included age, sex, pathology, tumor stage; the method of diagnosis; location of primary lesion (central, peripheral, or intermediate); tumor size, mediastinal lymph node metastasis, and the serum carcinoembryonic antigen (CEA) value. The CEA was detected in 96 serum samples using enzyme-linked immunosorbent assays.

Methods

Various Olympus electronic bronchoscopes (Japan) were used for performing the procedures, and the bronchoscopies were performed in accordance with the standard protocols. Briefly, the bronchoscopies were performed orally, and 2% lidocaine was administered as the anesthetic. In all cases, a full inspection of the tracheobronchial tree was performed. After the inspection, the lesion was localized using HRCT, and forceps were inserted to conduct TBLB at the nearest bronchial mucosa to the lesion (2–3 samples). Subsequently, bronchial brushing and bronchoalveolar lavage (BAL) were performed. The results of the transbronchial needle aspiration were not included in the analyses.

All patients signed informed consent forms before endoscopy. The ethics committee of our institution approved the study.

Statistical analysis

All data were analyzed using the SPSS software version 22 (SPSS Inc., USA). The Pearson chi-square test or Fisher's exact and McNemar tests were used in the univariate and multivariate analyses. A P value < 0.05 was considered statistically significant.

Table 3 Comparisons between the positive detection rates of different groups by bronchoscopy

Features	Total	Positive		χ^2	*P*
		n	%		
Sex					
Male	64	25	39.1	1.81	0.178
Female	45	12	26.7		
Pathology					
Adenocarcinoma	93	29	31.2	2.149	0.143
Squamous carcinoma	11	5	45.5		
SCLC	3	2	66.7		
Other	2	1	50.0		
Location					
Central	11	7	38.9	1.105	0.575
Intermediate	18	5	45.5		
Peripheral	80	25	31.3		
T stage					
T1–2	75	25	33.3	0.040	0.841
T3–4	34	12	35.3		
N stage					
N0–1	52	15	28.8	1.153	0.283
N2–3	57	22	38.6		
CEA value					
Positive	34	10	29.4	0.364	0.546
Negative	62	22	35.5		
Missing	13				

SCLC, small cell lung cancer

Results

In total, 109 patients were enrolled between January 2008 and December 2012, including 64 (58.7%) men and 45 (41.3%) women with a mean age of 58.4 years (range, 18–82 years). Herein, 93 out of 109 patients had adenocarcinoma (85.3%), 11 had squamous carcinoma (10.1%), and only 3 had small cell lung cancer (2.8%). The locations of the lesions were central in 11 (10.1%) cases, peripheral in 80 (73.4%), and intermediate in 18 (16.5%) cases (Table 1).

Of the 109 patients, 37 (33.9%) were diagnosed bronchoscopically, 34 (31.2%) by brushing and BAL, and 21 (19.3%) by biopsy. Brushing and BAL were identified to have higher positive detection rates than biopsy on the McNemar test ($P = 0.004$; Table 2). There were no statistically significant differences in the positive detection rates between the sex, pathology, lesion location, tumor size, lymph node metastasis, and the serum CEA value ($P > 0.05$ for all groups; Table 3)

Patients without a bronchoscopically confirmed diagnosis were diagnosed with another method. Twenty-nine cases (26.6%) were confirmed by transthoracic biopsy,

Table 4 The method used in the confirmation of diagnosis

Methods	Positive	
	n	%
Bronchoscope	37	33.9
Transthoracic biopsy	29	26.6
Pleural fluid	16	14.7
Surgery	26	23.9
Sputum	1	0.9

16 cases (14.7%) through analysis of the pleural fluid, 26 cases (23.9%) by surgery, and one case (0.9%) through sputum analysis (Table 4).

Of the 109 patients, none experienced uncontrollable bleeding after undergoing the standard procedures of brushing, BAL, and biopsy. Only 7 patients experienced slight bleeding, which was effectively managed using topical adrenaline.

Discussion

Lung cancer is the most common cause of cancer-related deaths worldwide, and most patients are diagnosed at an advanced stage [2]. Along with the extensive application of low-dose helical CT for screening lung cancer [3–5], the detection rates of solitary pulmonary nodules (SPNs) increased. The most common methods used in the diagnosis of SPNs are bronchoscopy, transthoracic needle aspiration, and surgical biopsy [6]. The diagnostic rate of malignant lesions by traditional TBLB ranged 14–63%, depending on the size and location of the lesions, and the skill and experience of the bronchoscopist [7]. There have been several developments in bronchoscopic technologies in order to improve diagnostic yields, including radial probe endobronchial ultrasonography, and in navigation systems, including electromagnetic navigation bronchoscopy and virtual bronchoscopy [8]. Despite the availability of several bronchoscopic approaches, TBLB, and brushing and BAL through bronchoscopy are still the most widely used techniques for diagnosis. Common bronchoscopy is used even more extensively because of its safety, convenience, and cost-effectiveness. However, studies seldom show the percentages when lesions are not detected by bronchoscopy [9–10]. Nowadays, biopsy specimens have become increasingly important for clinicians. It was reported that 87% of adenocarcinoma patients harbor driver gene mutations [11]. Biopsy specimens are required for the detection of these mutations, particularly for adenocarcinoma.

In this study, out of the 109 cases of undetectable endobronchial lesions, most involved adenocarcinoma (85.3%) and/or were peripheral lesions (73.4%). Consistent with previous studies, the total positive detection rate was 33.9% (37/109) [9–10]. Among the adenocarcinoma cases, 29 (31.2) showed positive results through TBLB, brushing, or BAL. Although the positive detection rate was not as high as that for other pathologies (45.5–66.7%), no statistically significant differences between them were observed. It is necessary to perform brushing and biopsy, because the incidence of adenocarcinoma was high in the whole lung cancer group and in patients who had lesions undetectable by bronchoscopy.

Brushing and BAL had significantly higher diagnostic positive detection rates than biopsy (31.2% vs. 19.3%, $P = 0.004$; Table 2). This might be because brushing and BAL could be performed within a much larger range, whereas only a small specimen could be obtained by biopsy with a rather limited range. The combination of biopsy with brushing and BAL could slightly increase the diagnostic positive detection rate of bronchoscopic examination.

There were no differences in the diagnostic positive detection rates according to sex, pathology, lesion location, tumor size, lymph node metastasis, and the serum CEA value. It appears that the positive detection rate does not relate to clinical factors. For example, the location of the lesions did not influence the positive detection rates. Furthermore, we investigated whether mediastinal lymph node metastasis affected the positive detection rates and found that mediastinal lymph node metastasis and hilar lymph node metastasis did not differ in their positive detection rates. We suggest this could primarily be because of the insufficient number of cases for obtaining positive results, and secondly, because the clinical factors evenly and dispersedly influenced the positive detection rates, which indicated any element could not have a statistically significant influence on the positive detection rates. In fact, as long as cancer cells invaded the bronchial mucosa, positive results could be obtained by biopsy or brushing, although no lesions were visible to the naked eye.

Of the 109 patients, none experienced uncontrollable bleeding after undergoing the standard procedure of brushing, particularly for biopsy. Therefore, biopsy is a sufficiently safe option for patients with lesions undetectable by bronchoscopy.

In conclusion, normal endobronchial manifestations could indicate lesions undetectable by bronchoscopy. Therefore, we suggest that endoscopists perform biopsy, brushing, and BAL. In addition to their safety, brushing and BAL might increase the positive detection rates by bronchoscopic examination.

Conflicts of interest

The authors indicated no potential conflicts of interest.

References

1. Ikeda S, Yanai N, Ishikawa S. Flexible bronchofiberscope. Keio J Med, 1968, 17: 1–16.
2. Torre LA, Bray F, Siegel RL, *et al.* Global cancer statistics, 2012. CA

Cancer J Clin, 2015, 65: 87–108.
3. National Lung Screening Trial Research Team, Aberle DR, Adams AM, *et al*. Reduced lung cancer mortality with low-dose computed tomographic screening. N Engl J Med, 2011, 365: 395–409.
4. Aberle DR, DeMello S, Berg CD, *et al*. Results of the two incidence screenings in the National Lung Screening Trial. N Engl J Med, 2013, 369: 920–931.
5. Liang M, Tang W, Xu DM, *et al.* Low-dose CT screening for lung cancer: computer-aided detection of missed lung cancers. Radiology, 2016, 28: 150063.
6. Krochmal R, Arias S, Yarmus L, *et al.* Diagnosis and management of pulmonary nodules. Expert Rev Respir Med, 2014, 8: 677–691.
7. Fukusumi M, Ichinose Y, Arimoto Y, *et al*. Bronchoscopy for pulmonary peripheral lesions with virtual fluoroscopic preprocedural planning combined with EBUS-GS: a pilot study. J Bronchology Interv Pulmonol, 2016, 23: 92–97.
8. Wang Memoli JS, Nietert PJ, Silvestri GA. Metaanalysis of guided bronchoscopy for the evaluation of the pulmonary nodule. Chest, 2012, 142: 385–393.
9. Botana-Rial M, Núñez-Delgado M, Pallarés-Sanmartín A, *et al*. Multivariate study of predictive factors for clearly defined lung lesions without visible endobronchial lesions in transbronchial biopsy. Surg Endosc, 2010, 24: 3031–3036.
10. Chechani V. Bronchoscopic diagnosis of solitary pulmonary nodules and lung masses in the absence of endobronchial abnormality. Chest,1996,109: 620–625.
11. Seo JS, Ju YS, Lee WC, *et al.* The transcriptional landscape and mutational profile of lung adenocarcinoma. Genome Res, 2012, 22: 2109–2119.

DOI 10.1007/s10330-016-0148-6
Cite this article as: Zheng H, Lu BH, Wang QH, *et al*. Bronchoscopic biopsy for diagnosis of lung cancer in the absence of visible endobronchial abnormalities. Oncol Transl Med, 2016, 2: 115–118.

Oncology and Translational Medicine
DOI 10.1007/s10330-015-0124-6

June 2016, Vol. 2, No. 3, P119–P126

ORIGINAL ARTICLE

Targeting of RhoE inhibits epithelial-mesenchymal transition during colorectal cancer cell migration

Gantao Chen[1, 2], Weiguo Dong[1] (✉)

[1] Department of Gastroenterology, Renmin Hospital of Wuhan University, Wuhan 430060, China
[2] Department of Gastroenterology, The third Renmin Hospital of Xiantao City, Xiantao 433000, China

Abstract

Objective Despite microRNA (miR-200b) being proved to promote the proliferation of colorectal cancer (CRC) cells, the relationship between miR-200b and epithelial-mesenchymal transition (EMT) of CRC cells remains poorly understood. The aim of the study was to investigate the relationship between miR-200b and EMT during CRC cell migration.

Methods The effect of miR-200b on EMT-associated markers E-cadherin and vimentin was evaluated by western blot in CRC cells (SW620 and HT-29) by treatment with miR-200b mimics and inhibitors. A luciferase reporter assay was employed to detect downstream targets of miR-200b. Transwell migration assays were used to detect CRC cell migration.

Results Western blots revealed that treatment with miR-200b mimics led to up-regulation of E-cadherin and down-regulation of vimentin, metalloproteinase (MMP)-9, and MMP-2, whereas treatment with miR-200b inhibitor exhibited opposite effects on expression of E-cadherin and vimentin. Luciferase reporter assays demonstrated that RhoE (RND3) was targeted by miR-200b. Two predicted target sites of miR-200b were present in the 3'-UTR of RhoE. Predicted target site 1 was from nucleotides 1584 to 1591, and site 2 was from nucleotides 1729 to 1735. RhoE knockdown cell lines were also established to investigate the impact of RhoE and miR-200b on EMT and cell migration. RhoE knockdown enhanced the effect of miR-200b mimics, up-regulating E-cadherin and down-regulating vimentin. RhoE knockdown also inhibited cell migration. Furthermore, miR-200b mimic treatment further promoted the inhibitory effect of RhoE knockdown on cell migration.

Conclusion miR-200b inhibited EMT and CRC cell migration partly via inhibiting RhoE expression in CRC. RhoE and miR-200b might therefore be promising target genes in the management of CRC.

Key words: miR-200b; colorectal cancer (CRC); metalloproteinase (MMP); epithelial-mesenchymal transition (EMT); cell migration

Received: 14 December 2015
Revised: 18 March 2016
Accepted: 25 April 2016

Colorectal cancer (CRC) is one of most common cancers and the fourth leading cause of cancer-related death worldwide [1]. Metastasis is the most common reason for the death of CRC patients [2]. Despite application of screening strategies, such as fecal occult-blood test, sigmoidoscopy and colonoscopy, approximately 500 000 patients with CRC die due to uncontrolled cancer metastasis each year [3]. Therefore, the molecular mechanisms of CRC metastasis and therapies focusing on specific molecular targets of CRC metastasis attract wide attention.

Epithelial-mesenchymal transition (EMT) is essential for initiation of cancer metastasis. In breast cancer, ovarian cancer, esophageal cancer, and colon cancer models, EMT has been observed. It has been established that EMT is aberrantly reactivated in tumor progression and contributes to cancer invasion and metastasis *in vivo* and *in vitro* [4]. Key features of EMT include deficiency of epithelial cell markers such as E-cadherin, and elevated expression of mesenchymal proteins such as vimentin [5–6]. Recent studies have demonstrated that E-cadherin also can be regulated by micro-RNAs [4]. It is established that microRNAs (miRNA) are a class of small noncoding gene-regulatory RNAs, which are involved in regulation of expression of cancer-related genes, and play roles in cancer invasion and metastasis [7–8]. Among miRNAs, miR-200b is a member of the miR-200 family. A large amount of

✉ Correspondence to: Weiguo Dong. Email: 415100331@qq.com

evidence supports the notion that miR-200b is associated with EMT of cancer cells. For instance, miR-200b is reported to suppress EMT and promote proliferation of intestinal epithelial cells [9]. It has been reported that miR-200b targets E-box-binding homeobox (ZEB) 1, which is involved in regulation of E-cadherin expression in gastric carcinoma [10]. Although it has been demonstrated that miR-200b promotes CRC cell proliferation through suppressing reversion-inducing cysteine-rich protein with Kazal motifs (RECK) [11], the relationship between miR-200b and EMT of CRC cells remains undefined. Here, we sought to reveal the role of miR-200b in EMT and CRC cell migration, and the potential underlying molecular mechanisms.

Rho proteins are important signaling molecules as a member of Rnd subfamily. Although RhoE lacks GTPase activity, it can bind GTP. These features give RhoE many unique functions that are different from other members of Rho family [12]. In recent years, it has been confirmed that Rho proteins show abnormal expression in many malignancies, such as colorectal cancer, breast cancer, stomach cancer, HCC, and pancreatic cancer. It has also been found that abnormal expression of Rho proteins was closely related to the tumor occurrence，invasion and metastasis [13]. Bioinformatic predictions have suggested that RhoE may be a target gene of miR-200b. However, there are few reports about the relationship between RhoE and miR-200b.

In this study, we studied the impact of miR-200b on the EMT-associated markers E-cadherin and vimentin in the colorectal cancer cell lines SW620 and HT-29, by treating the cells with miR-200b mimics and inhibitors. We also identified that miR-200b can inhibit EMT by regulating RhoE expression. Luciferase reporter assays were employed to detect downstream targets of miR-200b. We also investigated the impact of RhoE and miR-200b on cell migration. This study provides more clues regarding the molecular mechanism of miR-200b in CRC, and identifies novel targets of colon cancer treatment.

Materials and methods

Cell culture

Human CRC cell lines SW620 and HT-29 were obtained from American Type Culture Collection (ATCC, Manassas, VA, USA). All cell lines were cultured in Dulbecco's modified Eagle's medium (DMEM, Invitrogen, CA, USA), supplemented with penicillin (100 U/mL, Gibco, CA, USA), streptomycin (100 μg/mL, Gibco, CA, USA) and 10% fetal bovine serum (FBS) in an humidified incubator (37 ℃, 5% CO_2).

Cell transfection

For cell transfection, miR-200b mimics, miR-200b inhibitors, and a negative control were designed by and purchased from RiBoBio Company (Guangzhou, China). Transfections of miRNAs were performed using Lipofectamine2000 (Invitrogen, CA, USA) according to the manufacturer's protocol. After 6 hours, the culture medium was replaced with fresh DMEM. Total RNA and protein were prepared 48 hours after cell transfection for analysis by qRT-PCR or western blot, respectively.

Western blot

Western blotting was performed in accordance with standard procedures. Briefly, whole proteins were obtained from cell pellets lysed in RIPA buffer (Santa Cruz, USA) after required treatments, and were separated on 10% SDS-PAGE gels. The proteins were transferred onto PVDF membranes (Millipore, USA) which were blocked 1 h with 5% skim milk at room temperature (25 ℃) and incubated with primary antibodies overnight at 4 ℃. E-cadherin antibody was purchased from BD Bioscience (USA). Vimentin antibody, MMP-2 antibody, MMP-9, and GAPDH antibodies were purchased from Cell Signaling Technology (USA). RhoE antibody was purchased from R&D System. After washing with TBST (TBS + 0.1% TWEEN-20) three times, the membranes were incubated with horseradish peroxidase-conjugated secondary antibodies (Santa Cruz, USA) for 60 minutes at room temperature. Signals were visualized using the ECL system (Millipore, USA). GAPDH was detected as an internal control. Protein expression levels were quantified using ImageJ software (National Institute of Health, MA, USA) [14].

Quantitative real-time PCR

Total RNA, including miRNAs, was isolated from cells using TRIzol reagent (Invitrogen, USA) after required treatments according to the manufacturer's instructions. From 2.0 μg of total RNA, complementary DNA (cDNA) was randomly primed in a final volume of 20 μL using the RevertAid™ First Strand cDNA Synthesis Kit (Fermentas, Canada). Human GAPDH was amplified as an internal control. Quantitative real time-PCR reaction was conducted using ABI SYBR Green Master Mix (Applied Biosystems). Quantitative PCR (95 ℃ for 10 min, 40 cycles of 95 ℃ for 15 s, and 60 ℃ for 1 min) was performed with the ABI Step OnePlus™ system (Applied Biosystems). For miRNA analysis, real time PCR was performed as above. All miRNA data were expressed relative to a U6 small nuclear (sn) RNA (RiBoBio Company, Guangzhou, China). The $2^{-\Delta\Delta Ct}$ method was employed to process the data relative to U6 or GAPDH.

The PCR primer sequences were: RhoE: Forward: 5'-ATAGAGTTGAGCCTGTGGGACAC-3'; Reverse: 5'-AGGGTCTCTGGTCTACTGATGTC-3'; GAPDH: Forward: 5'-TGCACCACCAACTGCTTAGC-3'; Reverse: 5'-

GGCATGGACTGTGGTCATGAG-3'.

miRNA target prediction and Luciferase reporter assay

miR-200b targets were predicted based on miRanda (http://www.microrna.org), TargetScan (http://www.Targetscan.org), and PITA (http://genie.weizmann.ac.il/pubs/mir07) [15–17]. Many different target genes were predicted. Among these targets, we focused on one gene, RhoE (*RND3*), which has been shown to have a major role in the control of the actin cytoskeleton, influencing migration by changing cell motility [18].

A luciferase reporter assay was employed to validate whether RhoE was the direct target gene of miR-200b. The 3'-UTRs of RhoE were amplified by PCR using human genomic DNA. These were cloned into the *XhoI* site downstream of the luciferase coding region in the pGL3 vector (Promega, Madison, WI, USA). A pGL3 construct containing 3'-UTRs of RhoE with mutant seed sequences of miR-200b was also synthesized. For the luciferase assay, human HEK293T cells were seeded in DMEM supplemented with 10% FBS in 96-well plates and transfected with either pGL3 or pGL3-miR-200b vector (100 ng) and wild type or mutant 3'-UTR of RhoE (10 ng) using Lipofectamine-2000. Cells were harvested 48 hours after transfection. The Dual-Luciferase reporter assay system (Promega, WI, USA) was utilized for luciferase activity assay. All experiments were performed 3 times and the relative reporter activity was obtained following normalization to Renilla control luciferase activity.

Establishment of RhoE knockdown stable cell lines

To establish stable RhoE knockdown cell lines, SW620 and HT-29 cells were seeded in 6-well plates and transduced with RhoE-knockdown- or negative-control-lentiviruses (GenePharma, Shanghai, China). Lentiviral infection was carried out according to operation instructions.

Immunofluorescence assay

The cells were fixed with 4% paraformaldehyde, blocked with 3% bovine serum albumin (BSA) for half an hour, and then incubated with anti-E-cadherin primary antibody for 2 hours at room temperature. After rinsing washing times with PBS, the cells were incubated with second antibody conjugated with fluorescein isothiocyanate (FITC) for 1 hour at room temperature. Subsequently, the nuclei were counterstained with DAPI. Images were captured under a fluorescent microscope (Olympus BX51, Olympus, Japan) and analyzed using ImageJ software (National Institute of Health, MA, USA) [14].

Cell migration assay

For migration assay, Transwell migration chambers with 8 μm pore size (Corning, NY, USA) were used. Briefly, suspended cells in serum-free medium (1×10^5) were placed on each upper chamber, and 500 μL medium with 10% FBS was added to the bottom chamber in a 5% CO_2 humidified incubator. After incubation for 24 hours at 37 ℃, the cells on the upper surface of the trans-well membrane were removed using a cotton swab. The migrated cells on the reverse side were fixed in methanol, stained with crystal violet and photographed under a microscope (100 × magnification). Six random fields from each triplicate membrane were imaged and the number of migrant cells counted for each experimental group.

Statistical analysis

All data were expressed as mean ± SEM. The difference among treatment groups was analyzed by Student's *t*-test or one-way ANOVA followed by Student-Newman-Keuls (SNK) test (SPSS 19.0 statistical software). *P*-value < 0.05 was regarded statistically significant.

Results

miR-200b regulated expression of E-cadherin and vimentin in CRC cells

Loss of E-cadherin expression and increased vimentin expression are important markers of EMT. To validate whether miR-200b regulates EMT of CRC cells, we characterized the expression levels of E-cadherin and vimentin in SW620 and HT-29 cell lines by transfecting with miR-200b mimics, miR-200b inhibitors, or miR-n.c. (negative control). As shown in Fig. 1, overexpression of miR-200b (treatment with miR-200b mimics) led to up-regulation of E-cadherin and down-regulation of vimentin compared to negative control in SW620 and HT-29 cell lines ($P < 0.05$). Moreover, transfection with miR-200b inhibitor resulted in reduction of E-cadherin and elevation of vimentin ($P < 0.05$). These data showed that miR-200b regulates the expression of E-cadherin and vimentin, and inhibited EMT of CRC cells.

Metalloproteinase (MMP)-9 and MMP-2 are involved in ECM remodeling and angiogenesis and associated with cancer progression [19]. We also investigated the effects of miR-200b on MMP-2/9 in our study. We found that MMP-9 and MMP-2 were dramatically decreased in CRC cells after transfection with miR-200b mimics ($P < 0.05$). On the contrary, miR-200b inhibitor treatment significantly increased the expression MMP-9/2 protein ($P < 0.05$), suggesting that miR-200b also regulates the expression of MMP-9/2.

miR-200b targeted RhoE

Using online miRNA target prediction databases (Targetscan, miRNA.org and PITA), we predicted a great number of target genes of miR-200b. Among these target

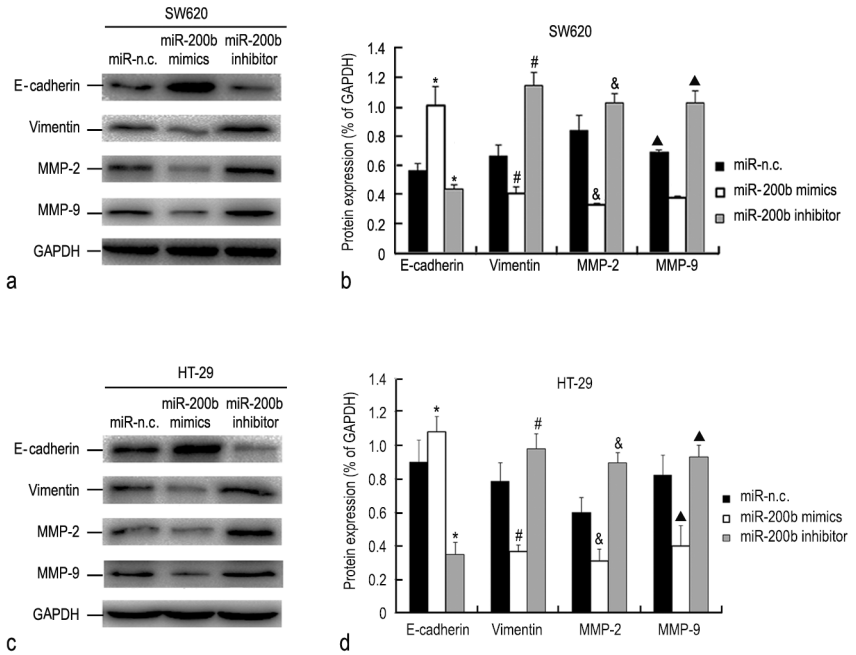

Fig. 1 Effect of miR-200b on E-cadherin, vimentin, MMP-2 and MMP-9 in SW620 and HT-29 cells. (a and c) SW620 and HT-29 cells were transfected with miR-200b n.c., miR-200b mimics and miR-200b inhibitor. Western blot analysis detected protein expression of E-cadherin, vimentin, MMP-2, MMP-9 and control GAPDH protein levels. (b and d), Densitometry analysis of E-cadherin, vimentin, MMP-2 MMP-9 and control GAPDH protein levels in SW620 and HT-29 cells. * $P < 0.05$, compared with negative control of E-cadherin; # $P < 0.05$, compared with negative control of vimentin; & $P < 0.05$, compared with negative control of MMP-2; ▲ $P < 0.05$, compared with negative control of MMP-9

genes, we identified on RhoE, which is involved in cell motility and migration [20]. To validate whether RhoE was the direct target gene of miR-200b, we cloned luciferase reporter vectors containing the full length 3'-UTR of RhoE. Relative luciferase activity was significantly suppressed in HEK293T cells co-transfected with miR-200b and wild type 3'-UTR of RhoE ($P < 0.05$, Fig. 2). The data confirm that RhoE is the target gene of miR-200b.

Moreover, as shown in Fig. 2a, we also identified two predicted target sites of miR-200b: the site 1 was from nucleotides 1584 to 1591, and site 2 was from nucleotides 1729 to 1735 in 3'-UTR of RhoE. To analyze which predicted site was targeted by miR-200b, we generated a wild type RhoE 3'-UTR reporter construct and 2 mutated RhoE 3'-UTR reporter constructs. The first one contained predicted target site 1 and the second one contained site 2. As shown in Fig. 2b, luciferase activity was significantly suppressed in HEK293T cells co-transfected with miR-200b and the wild type 3'-UTR of RhoE. In contrast, the first mutant reporter construct led to a smaller decrease in luciferase activity in miR-200b-transfected HEK293T cells ($P < 0.05$). The second mutant reporter construct led to slightly decreased luciferase activity in miR-200b-transfected HEK293T cells, although this did not reach statistical significance (Fig. 2b, $P > 0.05$). These results reveal that both predicted target site 1 and 2 in 3'-UTR of RhoE are target sites of miR-200b.

The effect of miR-200b on endogenous expression of RhoE was subsequently examined by western blot (Fig. 3) in CRC cells lines. Transfection of miR-200b mimics resulted in a strong decrease of RhoE protein in SW620 and HT-29 cells ($P < 0.05$). However, transfection of miR-200b inhibitor up-regulated RhoE expression ($P < 0.05$). These findings demonstrate that miR-200b negatively regulates the RhoE expression.

RhoE knockdown inhibits EMT in CRC cell lines

Next, to test whether RhoE expression affected miR-220b regulated EMT in SW620 and HT-29 cells, we knocked down the expression of RhoE in SW620 and HT-29 cells. As shown in Fig. 4, the expression level of RhoE was significantly reduced in RhoE-knockdown cells compared to the negative control in the two cell lines ($P < 0.05$). RhoE knockdown resulted in increased E-cadherin and decreased vimentin expression ($P < 0.05$). Furthermore, miR-200b mimic transfection in RhoE-knockdown cells resulted in further down-regulated RhoE, up-regulated E-cadherin and down-regulated vimentin expression compared to the negative control ($P < 0.01$). The results in SW620 and HT-29 cell lines were consistent.

Immunofluorescence labeling with an anti-E-cadherin antibody demonstrated similar results (Fig. 3b). When RhoE expression was silenced in SW620 cells, E-cadherin expression was markedly increased compared with the negative control. Furthermore, miR-200b mimic transfection led to more obviously decreased E-cadherin expression in RhoE-knockdown SW620 cells. Taken together, these data demonstrate that RhoE expression was negatively regulated by miR-200b, which might regulate EMT process by targeting RhoE.

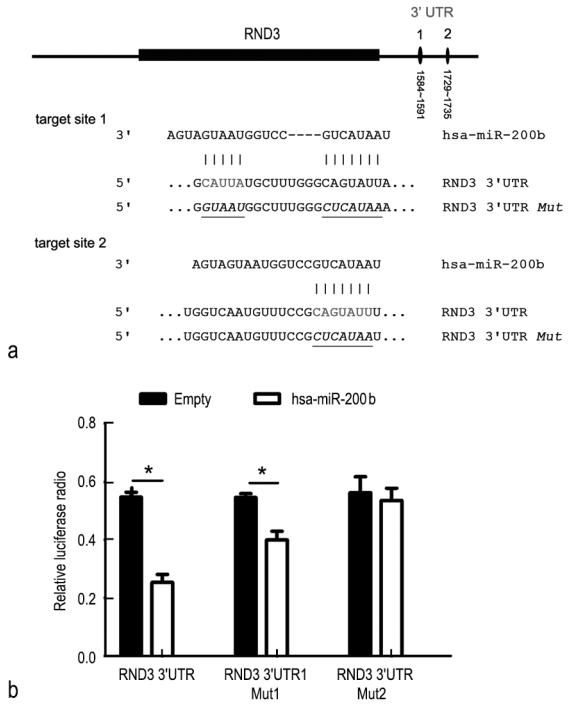

Fig. 2 miR-200b targets RhoE. (a) Two putative binding sites of miR-200b at position of 1584–1591 and 1729–1735 regions in RhoE 3'-UTR region were predicted by TargetScan. The mutated versions by sites mutagenesis were also shown. (b) Effect of 2 mutated RhoE 3'-UTR reporter constructed on luciferase activity. Luciferase reporter assay detected the luciferase activity in HEK293T cells co-transfected with miR-200b, and wild type or mutant 3'-UTR of RhoE. * $P < 0.05$, compared with negative control

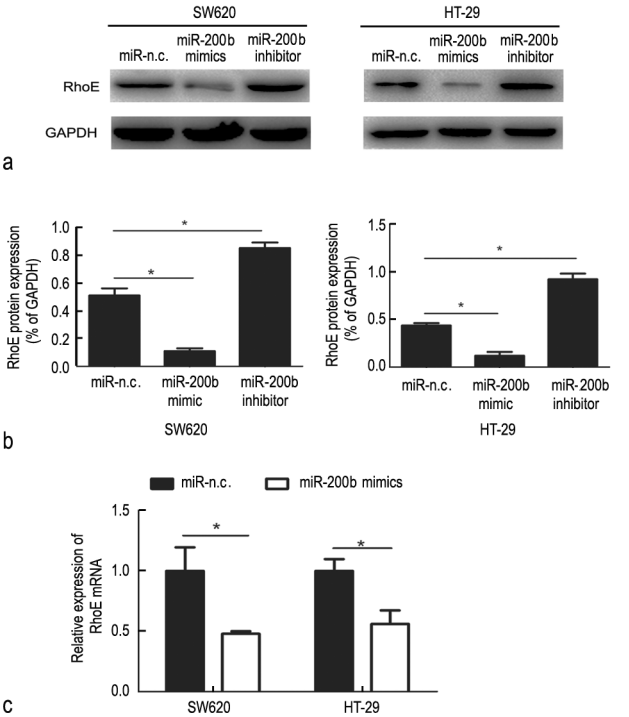

Fig. 3 Effect of miR-200b on endogenous expression of RhoE in SW620 and HT-29 cells. (a) Detecting the protein expression of RhoE in SW620 and HT-29 cells transfected with miR-200b-n.c., miR-200b mimics and miR-200b inhibitor by western blot. (b) Densitometry analysis of RhoE protein in SW620 and HT-29 cells transfected with miR-200b-n.c., miR-200b mimics and miR-200b inhibitor, respectively. RhoE protein was significantly down-regulated by miR-200b mimics, but was elevated by miR-200b inhibitors. * $P < 0.05$, compared with miR-n.c. (c) Detecting the expression of RhoE mRNA in SW620 and HT-29 cells transfected with miR-n.c. and miR-200b mimics, respectively. * $P < 0.05$, compared with miR-n.c.

Reduced miR-200b levels induced EMT in result of control CRC cells migration

We further investigated the influence of miR-200b and RhoE on CRC cell migration by using trans-well migration assay. As shown in Fig. 5, we found that miR-200b inhibitor transfection of SW620 cells promoted cell migration compared to negative control ($P < 0.05$). RhoE knockdown dramatically decreased SW620 cell migration compared to the negative control ($P < 0.05$), indicating that down-regulation of RhoE expression suppresses cell migration. Moreover, treatment with miR-200b mimics further reduced migrated RhoE-knockdown-SW620 cells compared to the negative control transfected RhoE knockdown-SW620 cells ($P < 0.05$). Our data demonstrate that miR-200b overexpression and RhoE knockdown inhibit cell migration. miR-200b may suppress CRC cell migration by down-regulating RhoE.

Discussion

Cancer metastasis remains a primary reason of colorectal cancer-related mortality. EMT is recognized as the initiation step of cancer metastasis and is linked to malignant conversion of cancer cells [21]. EMT is characterized by the decreased E-cadherin and increased of vimentin expression. Although it is known that miR-200b, as a member of miR-200 family, is a powerful regulator of EMT in several cancer types, there little data regarding miR-200b in CRC. In the current study, we found that treatment of cells with miR-200b mimics led to up-regulation of E-cadherin and down-regulation of vimentin, whereas treatment of miR-200b inhibitor exhibited opposing effects on expression of E-cadherin and vimentin. We also found that miR-200b suppressed EMT of CRC cell. This finding is in agreement with a previous report showing that miR-200b suppresses EMT in intestinal epithelial cells [9].

MMP-9/2 play positive roles in remodeling of extracellular matrix and angiogenesis, thus they are closely associated with cancer progression [22–23]. MMP-9/2 have reported to be elevated in CRC tissue compared to normal

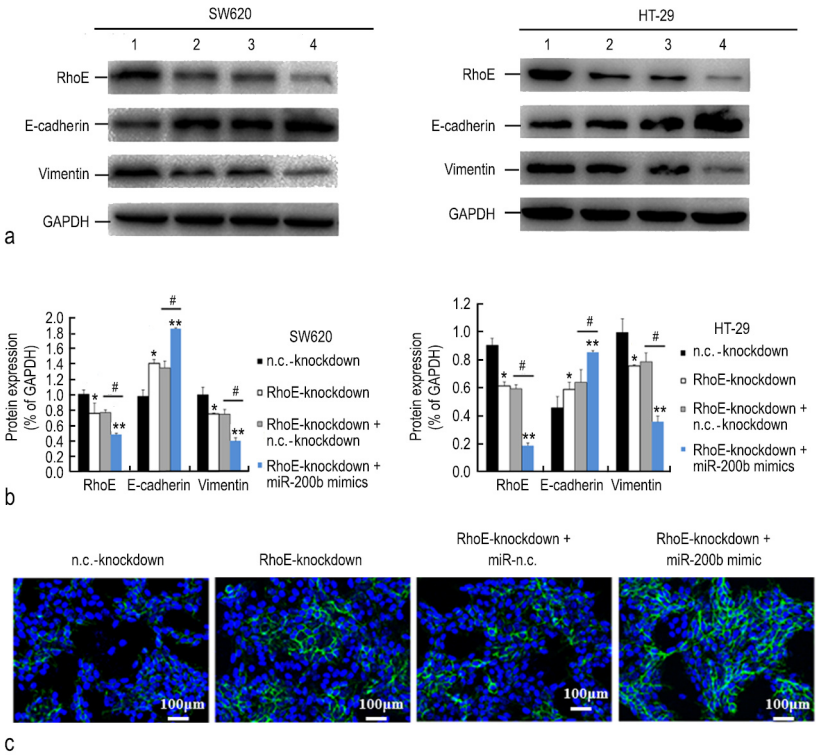

Fig. 4 Effect of RhoE silencing on E-cadherin and vimentin in SW620 and HT-29 cells. (a) Western blot analysis of RhoE, E-cadherin, vimentin after RhoE knockdown with lentivirus transfection. RhoE knockdown cells were transfected with miR-200b mimics or miR-200b n.c. (1, n.c.-knockdown; 2, RhoE-knockdown; 3, RhoE-knockdown + miR-n.c.; 4, RhoE-knockdown + miR-200b mimics). (b) Densitometry analysis of RhoE, E-cadherin and vimentin. * $P < 0.05$, ** $P < 0.01$, compared with negative control. (c) Immunofluorescent analysis with anti-E-cadherin antibody. RhoE knockdown SW620 cells were transfected with miR-200b mimics or miR-200b n.c. Expression of E-cadherin was observed by phase contrast microscopy (x 200)

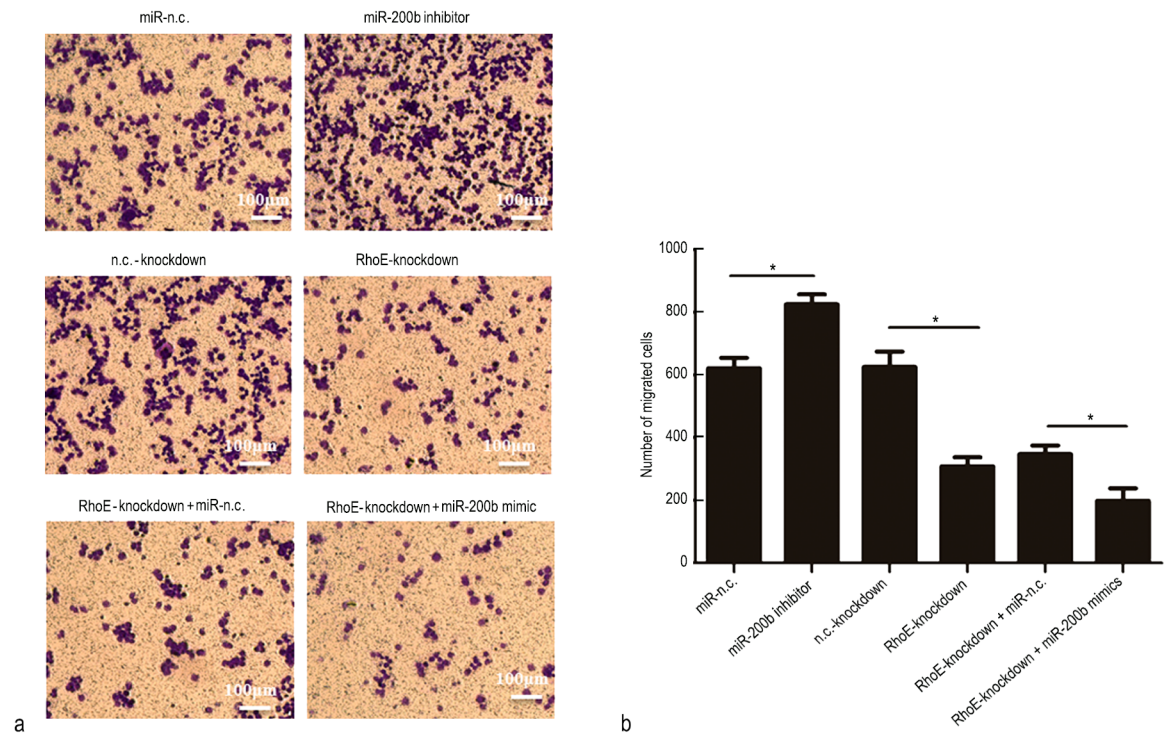

Fig. 5 Influence of miR-200b on migration of SW620 and HT-29 cells. (a) Transwell migration system was used to evaluate cell migration. The migrated cells were observed by phase contrast microscopy (x 100). (b) Quantitative analysis of average numbers of migrated cells for each condition. * $P < 0.05$, compared with negative control

tissue [24]. In our study, the expression of both MMP-9 and MMP-2 was decreased in response to miR-200b mimics, but were increased in response to miR-200b inhibitor treatment. This indicates that expression of MMP-9/2 might be negatively regulated by miR-200b, potentially preventing EMT via regulation of MMP-9/2.

RhoE, an atypical Rho protein, is intimately involved with cell migration [25–26]. Its expression is significantly correlated with cancer cell invasion, lymph node metastasis, and distant metastasis of CRC, and a poor prognosis for patients with CRC. Additionally, the positive rate of RhoE is higher in CRC patients than that in normal subjects [27]. Our study showed that RhoE is specifically targeted by miR-200b. In line with our observations, RhoE expression has been reported to be reduced by miR-200b transfection in HeLa cells [28]. Furthermore, we found two target sites of miR-200b in 3'-UTR of RhoE: site 1 from nucleotides 1584 to 1591, and site 2 from nucleotides 1729 to 1735.

Analysis of western blot results showed that miR-200b mimic transfection reduced RhoE expression to a greater extent in RhoE knockdown cells, confirming that miR-200b negatively regulates RhoE expression. Moreover, RhoE knockdown combined with miR-200b mimic transfection further up-regulated E-cadherin and down-regulated vimentin compared to treatment of miR-200b mimic transfection alone, as indicated by consistent results of western blot and immunofluorescence analysis. These findings reveal that miR-200b suppresses EMT of CRC cells by targeting RhoE.

It has been previously demonstrated that RhoE expression is reduced in CRC tissues compared to normal tissues and adenomas, and may function as a tumor suppressor gene to suppress CRC cell proliferation and growth [29]. Our study revealed that RhoE also prohibits cell migration, as indicated by the observation that RhoE knockdown decreases migration of SW620 cells. Furthermore, miR-200b mimic treatment promoted the effect of RhoE-knockdown to decrease migration of cells. Our findings indicate that miR-200b inhibits migration of cancer cells via down-regulating RhoE.

Our findings showed that miR-200b plays a suppressive role in EMT and cellular migration, at least in part by inhibiting expression of RhoE. There is evidence that RhoE inhibits invasion of cancer cells mediated by RhoA-ROCK (Rho-associated coil-containing protein kinase) pathway [30]. Moreover, overexpression of dominant-negative N-terminally truncated ROKα, functions as a downstream target for RhoA in induced cell spreading of HeLa and 3T3 cells [31]. These studies reveal that RhoA-ROCK and ROKα might be possible downstream targets of RhoE in CRC. More experiments are required to validate and extend the results of this study.

Conclusion

In summary, we provide *in vitro* evidence that miR-200b suppresses EMT and cell migration, via inhibition of RhoE expression in CRC. The study deepens our understanding of the role of miR-200b in CRC. These data collectively suggest that miR-200b and RhoE may serve as potential therapeutic targets to reduce CRC migration.

Conflicts of interest

The authors indicated no potential conflicts of interest.

References

1. Siegel R, Naishadham D, Jemal A. Cancer statistics, 2013. CA Cancer J Clin, 2013, 63: 11–30.
2. Wittekind C, Neid M. Cancer invasion and metastasis. Oncology 2005, 69 Suppl 1: 14–16.
3. Weitz J, Koch M, Debus J, *et al*. Colorectal cancer. Lancet, 2005, 365: 153–165.
4. Deng JJ, Xu XM. Epithelial-mesenchymal transition and cancermetastasis. Chinese-German J Clin Oncol, 2011, 10: 125–133.
5. Hirohashi S. Inactivation of the E-cadherin-mediated cell adhesion system in human cancers. Am J Pathol, 1998, 153: 333–339.
6. Hanahan D, Weinberg RA. Hallmarks of cancer: the next generation. Cell, 2011, 144: 646–674.
7. van Kouwenhove M, Kedde M, Agami R. MicroRNA regulation by RNA-binding proteins and its implications for cancer. Nat Rev Cancer, 2011, 11: 644–656.
8. Garzon R, Calin GA, Croce CM. MicroRNAs in cancer. Annu Rev Med, 2009, 60: 167–179.
9. Chen Y, Xiao Y, Ge W, *et al*. miR-200b inhibits TGF-beta1-induced epithelial-mesenchymal transition and promotes growth of intestinal epithelial cells. Cell Death Dis, 2013, 4: e541.
10. Kurashige J, Kamohara H, Watanabe M, *et al*. MicroRNA-200b regulates cell proliferation, invasion, and migration by directly targeting ZEB2 in gastric carcinoma. Ann Surg Oncol, 2012, 19 Suppl 3: S656–S664.
11. Pan Y, Liang H, Chen W, *et al*. microRNA-200b and microRNA-200c promote colorectal cancer cell proliferation via targeting the reversion-inducing cysteine-rich protein with Kazal motifs. RNA Biol, 2015, 12: 276–289.
12. Alberts SR, Cervantes A, van de Velde CJ. Gastric cancer: epidemiology, pathology and treatment. Ann Oncol, 2003, 14 Suppl 2: ii31–ii36.
13. Li FR, Jing H. Research progress of the relationship between Rho protein and malignant tumor. Int J Dig Dis (Chinese), 2014, 34: 52–55.
14. Abràmoff MD, Magalhães PJ, Ram SJ. Image processing with ImageJ. Biophoton Inter, 2003, 11: 36–42.
15. Mu P, Han YC, Betel D, *et al*. Genetic dissection of the miR-17 approximately 92 cluster of microRNAs in Myc-induced B-cell lymphomas. Genes Dev, 2009, 23: 2806–2811.
16. Betel D, Wilson M, Gabow A, *et al*. The microRNA.org resource: targets and expression. Nucleic Acids Res, 2008, 36 (Database issue): D149–D153.
17. Mazière P, Enright AJ. Prediction of microRNA targets. Drug Discov Today, 2007, 12: 452–458.
18. Tryndyak VP, Beland FA, Pogribny IP. E-cadherin transcriptional down-regulation by epigenetic and microRNA-200 family alterations

is related to mesenchymal and drug-resistant phenotypes in human breast cancer cells. Int J Cancer, 2010, 126: 2575–2583.
19. Zeng ZS, Cohen AM, Guillem JG. Loss of basement membrane type IV collagen is associated with increased expression of metalloproteinases 2 and 9 (MMP-2 and MMP-9) during human colorectal tumorigenesis. Carcinogenesis, 1999, 20: 749–755.
20. Guasch RM, Scambler P, Jones GE, *et al*. RhoE regulates actin cytoskeleton organization and cell migration. Mol Cell Biol, 1998, 18: 4761–4771.
21. Davalos V, Moutinho C, Villanueva A, *et al*. Dynamic epigenetic regulation of the microRNA-200 family mediates epithelial and mesenchymal transitions in human tumorigenesis. Oncogene, 2012, 31: 2062–2074.
22. Schmalfeldt B, Prechtel D, Härting K, *et al*. Increased expression of matrix metalloproteinases (MMP)-2, MMP-9, and the urokinase-type plasminogen activator is associated with progression from benign to advanced ovarian cancer. Clin Cancer Res, 2001, 7: 2396–2404.
23. Bergers G, Brekken R, McMahon G, *et al*. Matrix metalloproteinase-9 triggers the angiogenic switch during carcinogenesis. Nat Cell Biol, 2000, 2: 737–744.
24. Morán A, Iniesta P, García-Aranda C, *et al*. Clinical relevance of MMP-9, MMP-2, TIMP-1 and TIMP-2 in colorectal cancer. Oncol Rep, 2005, 13: 115–120.
25. Zhao H, Yang J, Fan T, *et al*. RhoE functions as a tumor suppressor in esophageal squamous cell carcinoma and modulates the PTEN/PI3K/Akt signaling pathway. Tumour Biol, 2012, 33: 1363–1374.
26. Riento K, Villalonga P, Garg R, *et al*. Function and regulation of RhoE. Biochem Soc Trans, 2005, 33: 649–651.
27. Zhou J, Yang J, Li K, *et al*. RhoE is associated with relapse and prognosis of patients with colorectal cancer. Ann Surg Oncol, 2013, 20: 175–182.
28. Xia W, Li J, Chen L, *et al*. MicroRNA-200b regulates cyclin D1 expression and promotes S-phase entry by targeting RND3 in HeLa cells. Mol Cell Biochem, 2010, 344: 261–266.
29. Luo H, Zou J, Dong Z, *et al*. Up-regulated miR-17 promotes cell proliferation, tumour growth and cell cycle progression by targeting the RND3 tumour suppressor gene in colorectal carcinoma. Biochem J, 2012, 442: 311–321.
30. Gadea G, de Toledo M, Anguille C, *et al*. Loss of p53 promotes RhoA-ROCK-dependent cell migration and invasion in 3D matrices. J Cell Biol, 2007, 178: 23–30.
31. Leung T, Chen XQ, Manser E, *et al*. The p160 RhoA-binding kinase ROK alpha is a member of a kinase family and is involved in the reorganization of the cytoskeleton. Mol Cell Biol, 1996, 16: 5313–5327.

DOI 10.1007/s10330-015-0124-6
Cite this article as: Chen GT, Dong WG. Targeting of RhoE inhibits epithelial-mesenchymal transition during colorectal cancer cell migration. Oncol Transl Med, 2016, 2: 119–126.

Oncology and Translational Medicine
DOI 10.1007/s10330-016-0156-6

June 2016, Vol. 2, No. 3, P127–P131

ORIGINAL ARTICLE

Modulation of MMP-2 and TIMP-2 by low dose radiation in mice bearing S180 sarcoma

Xiangmin Jia, Hongsheng Yu (✉)

Department of Oncology, The Affiliated Hospital of Qingdao University, Qingdao 266003, China

Abstract

Objective To investigate the inhibition of low dose radiation (LDR) on S180 sarcomas and its modulation of MMP-2 and TIMP-2 in mice.

Methods S180 subcutaneously implanted tumor model mice were randomly divided into two groups: control (N) and low dose radiation (LDR) groups. N mice were sacrificed after 12 h, whereas LDR mice were sacrificed after 12 (LDR-12 h), 24 (LDR-24 h), 48 (LDR-48 h), and 72 (LDR-72 h) h. Thereafter, we measured the tumor volumes. Histopathology was performed, and P-V immunohistochemistry was applied to assess MMP-2 and TIMP-2 expression.

Results Compared with the control group, the tumor growth was significantly inhibited in the LDR groups ($P < 0.05$). MMP-2 expression was considerably reduced in LDR-24h ($P < 0.05$) and LDR-48h ($P < 0.05$), whereas the change of TIMP-2 was not obvious in the LDR groups ($P > 0.05$) in contrast to that of the control group.

Conclusion LDR can effectively suppress the growth of S180 implanted tumors by reducing MMP-2, which is associated with invasion and metastasis.

Received: 30 March 2016
Revised: 26 April 2016
Accepted: 15 May 2016

Key words: MMP-2; TIMP-2; low dose radiation; S180 sarcoma

As a global public health problem, malignant tumors are becoming more common, resulting in a relatively high mortality rate and a negative effect on human health. Common treatments for malignant tumors include surgery, radiotherapy, chemotherapy, endocrine treatment, and biological immunotherapy. Tubiana (1999) reported that 45% of malignant tumors could be cured by surgery (22%), radiotherapy (18%), and drugs and other methods (5%). Thus, radiotherapy is very important in the treatment of malignant tumors [1]. However, radiation could damage various cellular components, directly (molecule ionization) or indirectly (reactive oxygen species production), including DNA. For protection, the irradiated cells may have innate defense mechanisms, such as the removal of oxidative stress and damaged cells, and DNA repair that may cause tissue or organ dysfunction and malignant diseases [2–3]. According to Muller's data, low doses of radiation can cause dose-proportional detrimental effects, such as cancer and heritable genetic mutations, without a threshold dose, which has been defined as the "linear-no-threshold (LNT) hypothesis". However, the accuracy of the LNT hypothesis for estimating cancer risks from low dose radiation by experimental and epidemiological evidence should be determined [2, 4]. The United Nations Scientific Committee on the Effects of Atomic Radiation (UNSCEAR) (1986) reported that LDR refers to a low linear energy transfer (LET) radiation dose of < 0.2 Gy or a high LET radiation dose of < 0.05 Gy, and the radiation dose rate should be > 0.05 mGy/min. Increasing experimental and clinical data has identified that LDR could induce comprehensive adaptive responses that could improve immunity and enhance the tolerance of normal tissue under radiation. In addition, pre-low-dose radiation for cells could increase their sensitivity to acute irradiation at high doses [5–6]. Low-dose hypersensitivity (HRS) eliminated potential mutant cells and reduced carcinogenic risks observed with LDR, and disappeared at doses > 0.5 Gy [2]. Global research has shown that LDR has shown positive results in the treatment of malignant tumors.

Tumor invasion and metastasis are processes involved with tumors cells and extracellular matrix components (ECM), which provide a significant barrier to tumor cell

✉ Correspondence to: Hongsheng Yu. Email: qdhsyu@126.com

invasion [7]. Numerous clinical and experimental studies have demonstrated that matrix metalloproteinases (MMPs), especially MMP-2 and MMP-9, play a key role in tumor cell invasion and metastasis due to their ability to degrade type IV collagen, a major component of the ECM [8]. As inactive pro-enzymes in a latent zymogenic form, MMP-2 and MMP-9 were activated by other MMPs or proteases and inhibited by specific inhibitors, and tissue inhibitors of metalloproteinases (TIMPs); and TIMP-2 specifically inactivated MMP-2. Consequently, the imbalance of MMP-2 and TIMP-2 may be the critical decisive factor for tumor progression and recurrence in cancer [7–8]. The overall aim of the present experiment was to study the relationship between LDR and MMP-2 and TIMP-2 expression, so that the antitumor mechanisms of LDR could be determined to provide an enhanced theoretical guide for its clinical application.

Materials and methods

Animals and chemicals

Male Kunming mice (purchased from Qingdao Institute for Drug Control, China), weight 20–22 g, 3–4 weeks old, were raised in specific pathogen free (SPF) conditions with unlimited food and water in a laminar flow clean bio-frame (License No. SCXK (Lu) 20030010). The monoclonal antibodies, MMP-2 (Bioss Biotechnology Co. Ltd) and TIMP-2 (Santa Cruz Biotechnology Co. Ltd) were rabbit anti-human immunoglobulin IgG1.

Cell lines and culture

S180 sarcoma cell lines were obtained from the Medical Pharmaceutical Research Institute, Shandong Province, China, and generated for 7 days in the abdomen of the mice. After S180 sarcoma cells were passaged intraperitoneally in two passages, the abdomen dropsy was drowned off to collect the tumor cells that were made into a single cell suspension of 6.5×10^7 mL. Later, we implanted 6.5×10^6 S180 sarcoma cells (0.1 mL) subcutaneously into the right inguen of the mice.

Radiation conditions

The tumor growth was observed when the mice were conventionally cultured with unlimited food and water for 7 days. Then, they were randomly divided into two groups: low dose radiation (LDR) and control (N). All the mice in the LDR group were exposed to 75 mGy of whole-body radiation via a cobalt-60 radiation machine (Xinhua Medical-equipment Company of Shandong Province). The mice were placed into wooden boxes (15 × 15 × 35 cm), and a lead plate (15 × 15 cm) was placed between the source and box to filter the radiation at a source skin distance of 160 cm, a radiation field of 45 × 45 cm, dose rate of 15.9 mGy/min, and exposure time of 4.72 min.

Specimen collection

Seven days after the mice were implanted with tumors, the maximum horizontal diameter, a (cm), and vertical diameter, b (cm), of the tumors were measured twice with a slide gauge to determine the average tumor size, and mice with tumors that were too large ($ab > 1.5$ cm^2) or too small ($ab < 0.40$ cm^2) were excluded. The formula of $V = 1/2\ ab^2$ was used to calculate the average tumor sizes. Mice in the LDR group were exposed to 75 mGy of whole-body radiation when there was no difference in the sizes of the tumors between the LDR and N groups. Then, the mice of the two groups were sacrificed at 12, 24, 48, and 72 h.

Tumor growth

The tumor tissue was exposed after the mice were sacrificed at 12, 24, 48, and 72 h, and the average volumes of tumors according to the above methods were calculated.

Detection of the MMP-2 and TIMP-2 level by PowerVision two-step immunostaining

(1) The tissues were fixed in 10% neutral formalin, and tumor cells were extracted using an automatic tissue hydroextractor, then flushed with water for at least 4 h and embedded in paraffin; (2) The tissues were sliced into 1–2 μm thick sections, and placed into a 60 °C thermotank overnight; (3) The paraffin sections were dewaxed with xylene, and hydrated with an ethanol gradient; (4) The sections were cooled at room temperature, and then placed into a potassium citrate solution (pH 6.0) in an autoclave for 5 min; (5) The sections were washed 3 times for 3 min each using a PBS buffer; (6) The sections were incubated for 80 min at 37 °C with the primary antibody (monoclonal antibodies of the rabbits); (7) The sections were washed 3 times for 3 min each using a PBS buffer; (8) The sections were incubated for 30 min at 37 °C with the second antibody; (9) The sections were washed 3 times for 3 min each using a PBS buffer; (10) The sections were dyed with a DAB stain; (10) The slides were washed with the running water, stained with hematoxylin and dehydrated with alcohol, then cleared in xylene and fixed in neutral balata. In addition, we replaced the primary antibody with a buffer as a negative control.

Semi-quantitative assay of MMP-2 and TIMP-2

The cells were counted using a high power microscope (× 200). According to the light or dark colors of the immunoreactive substances and the percentage of positive cells, the expression intensity of MMP-2 and TIMP-2 was divided into the following four categories: When the percentage of positive cells was < 5% , it was (–); when the positive cells were 5%–25% and the cells were slightly dyed, it was (+); when the positive cells were 26%–50% and tan particles were observed, it was (2+); when the

Table 1 Effects of low dose radiation on tumor growth (cm^3)

Group	*n*	Tumor volumes			
		12 h	24 h	48 h	72 h
N	0.3875 ± 0.26	0.3980 ± 0.31	0.4155 ± 0.33	0.5246 ± 0.36	0.7173 ± 0.35
LDR	0.3966 ± 0.22	0.3841 ± 0.30[a]	0.4037 ± 0.29[b]	0.4157 ± 0.31[c]	0.4108 ± 0.27[d]

[a] Compared with N, $t = 0.09$, $P > 0.05$; [b] Compared with N, $t = 0.08$, $P > 0.05$; [c] Compared with N, $t = 0.72$, $P > 0.05$; [d] Compared with N, $t = 2.19$, $P < 0.05$

positive cells were > 50% and stained stronger, it was (3+).

Statistical analysis

PPMS 1.5 was used for the statistical analysis. Quantitative data were expressed by mean ± standard deviation ($\chi \pm s$) and analyzed with a *t*-test. Semi-quantitative data were analyzed by Ridit scoring.

Results

The influence of LDR on the general condition of the mice

After receiving irradiation from 12 to 72 h, it was observed that the mice in the LDR groups were in a better mental state, more active, and ate more food than those in the N group.

The inhibition of tumor growth by LDR

After receiving low dose radiation, the tumor size was calculated at 12, 24, 48, and 72 h, as shown in Table 1. Compared with tumor size in the N mice, the tumor size of LDR mice was smaller, and there was a significant difference between the LDR-72 h and N groups ($P < 0.05$).

Effects of low dose radiation on MMP-2 and TIMP-2

The results showed that the MMP-2- and TIMP-2-positive stained cells that displayed granular brown substances in the cell membrane and cytoplasm were mainly tumor cells and interstitial cells adjacent to the tumor cells. The positive expression of MMP-2 and TIMP-2 was uneven with sheet and focal distributions. The data from the half-quantitative assay showed that MMP-2 expression was significantly different between LDR-24 h and LDR-48 h, and N ($P < 0.05$), whereas the variation in TIMP-2 was not obvious ($P > 0.05$) in contrast to N, as shown in Tables 2 and 3, and the microscopic observation (× 400) is shown in Fig. 1–4.

Table 2 The effects of LDR on MMP-2

Irradiation time (h)	Group	Counts				
		–	+	++	+++	Sum
12	N	1	5	4	0	10
	LDR-12 h	4	3	1	0	8[a]
24	N	1	5	4	0	10
	LDR-24 h	6	3	1	0	10[b]
48	N	1	4	4	1	10
	LDR-48 h	6	2	2	0	10[c]
72	N	2	6	2	0	10
	LDR-72 h	6	3	1	0	10[d]

[a] Compared with N, u = 1.86, $P = 0.06 > 0.05$; [b] Compared with N, u = 2.30, $P = 0.02 < 0.05$; [c] Compared with N, u = 2.15, $P = 0.03 < 0.05$; [d] Compared with N, u = 1.65, $P = 0.10 > 0.05$

Table 3 The effects of LDR on TIMP-2

Irradiation time (h)	Group	Counts				
		–	+	++	+++	Sum
12	N	3	4	3	0	10
	LDR-12 h	3	3	2	0	8[a]
24	N	2	4	3	1	10
	LDR-24 h	4	6	0	0	10[b]
48	N	3	4	3	0	10
	LDR-48 h	2	7	1	0	10[c]
72	N	2	5	1	1	10
	LDR-72 h	3	6	0	1	10[d]

[a] Compared with N, u = 0.33, $P = 0.74 > 0.05$; [b] Compared with N, u = 1.81, $P = 0.07 > 0.05$; [c] Compared with N, u = 0.29, $P = 0.77 > 0.05$; [d] Compared with N, u = 0.60, $P = 0.55 > 0.05$

Discussion

Recently, radiation has been used as a powerful tool in the therapy of malignant tumors, but high dose radiation can have harmful effects on normal cells [9]. The LNT hypothesis, which has been accepted by regulatory agencies worldwide, indicates that every radiation dose, no matter how low, is harmful to humans without a threshold. However, based on global data, especially Japanese A-bomb survivor data, it has been widely accepted that no statistically significant risk has been demonstrated in humans when exposed to doses < 100 mGy. Consequently, LDR could be used successfully in tumor treatment because of its ability to induce a stress response in cells, which reduces the risk of spontaneous and radiation-induced disease [9–11]. Extensive research shows that mammals, including humans, exposed to low-dose radiation can induce comprehensive adaptive responses, and reduce and suppress tumorigenesis. Nevertheless, the mechanism of tumorigenesis is unclear. It could be due to the activation of cell signaling, causing the production of a series of enzymes or proteins, regulating the expression of related genes, re-

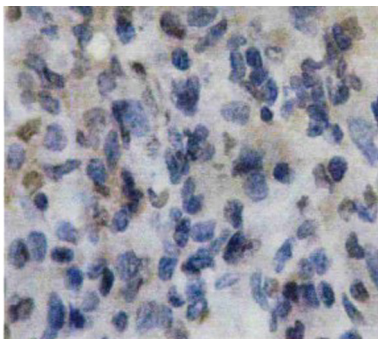

Fig. 1 The expression of MMP-2 in the control (N)

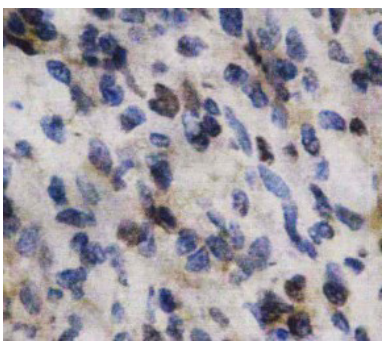

Fig. 2 The expression of MMP-2 in mice exposed to low dose radiation for 48 h (LDR-48 h)

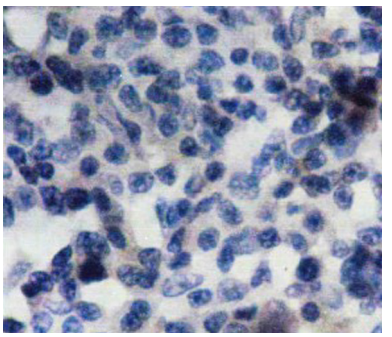

Fig. 3 The expression of TIMP-2 in the control (N)

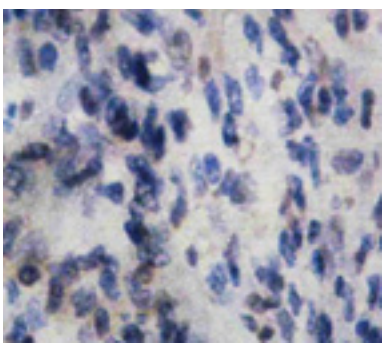

Fig. 4 The expression of TIMP-2 in mice exposed to low dose radiation for 48 h (LDR-48 h)

moving damaged cells through apoptosis, decreasing free radicals, and DNA repair after injured or increasing their sensitivity to acute irradiation at high doses [12–13].

Previous studies by our team found that LDR stimulated the growth of normal cells but not tumor cells *in vitro* and *in vivo* [6], and could reverse ovarian cancer cisplatin resistance by decreasing DNA damage repair and promoting apoptosis. Pre-chemotherapeutic LDR could induce anti-oxidative enzyme activities, and promote the elimination of free radicals to alleviate the damaging effects of oxidative stress to hepatic tissue caused by high-dose chemotherapeutics [14]. However, the relationship between LDR and cancer metastasis should be researched further.

The invasion and metastasis of neoplasm is a complex and multi-step continuous process that involves multiple genes, especially the MMP family. In this family, MMP-2 and MMP-9 have been widely studied and play an important role in ECM degradation. The TIMPs have the ability to block the function of MMPs, and the imbalance between MMPs and TIMPs is the principal cause of invasion and metastasis. As MMP-2, which could be specifically inhibited by TIMP-2, is closely related to the tumor invasion and metastasis [15–17] ,we examined the changes of MMP-2 and TIMP-2 expression after exposure to LDR to elucidate the relationship between LDR and cancer metastasis or invasion.

In the present study, we explored the effect of LDR on mice bearing S180 sarcomas by measuring the tumor volumes and detecting MMP-2 and TIMP-2 expression level by P-V immunohistochemistry. As expected, the results showed that tumor growth with LDR was significantly inhibited, and MMP-2 expression was considerably reduced in LDR-24 h and LDR-48 h. Therefore, LDR inhibited tumor growth and reduced MMP-2 expression. MMP-2 plays an important role in the invasion and metastasis of neoplasm, therefore, it is possible that LDR could inhibit tumor invasion and metastasis by reducing MMP-2 expression. Unfortunately, TIMP-2 expression varied after LDR exposure, but not significantly. It is possible that MMP-2 expression could be inhibited by factors other than TIMP-2, but this is unclear and further research is necessary to elucidate these relationships. However, this experiment provides a new mechanism where LDR could suppress tumor growth and inhibit tumor invasion and metastasis, which suggests that LDR would be suitable in clinical applications.

Conflicts of interest

The authors indicated no potential conflicts of interest.

References

1. Yu JM, Xing LG, Status and Prospects of Radiaton Oncology in China. China J Cancer Prev Treat, 2003, 10: 13–16.
2. Seong KM, Seo S, Lee D, *et al*. Is the linear no-threshold dose-response paradigm still necessary for the asessment of health effects of low dose radiation? J Korean Med Sci, 2016, 31: s10–23.
3. Goodhead DT. Understanding and characterisation of the risks to human health from exposure to low levels of radiation. Radiat Prot Dosimetry, 2009,137: 109–117.
4. Dauer LT, Brooks AL, Hoel DG, *et al.* Review and evaluation of updated research on the health effects associated with low-dose ionising radiation. Radiat Prot Dosimetry, 2010, 140: 103–136.
5. Wang SK, Jiang G, Yu HS, *et al.* Effect of low-dose X-ray radiation on adaptive response in gastric cancer cell. Chinese-German J Clin Oncol, 2013, 12: 171–174.
6. Yu H, Liu N, Wang H, Shang Q, *et al*. Different responses of tumor and normal cells to low-dose radiation. Contemp Oncol (Pozn), 2013, 17: 356–362.
7. Ricci S, Bruzzese D, DI Carlo A, *et al*. Evaluation of MMP-2, MMP-9, TIMP-1, TIMP-2, NGAL and MMP-9/NGAL complex in urine and sera from patients with bladder cancer. Oncol Lett, 2015, 10: 2527–2532.
8. Roomi MW, Kalinovsky T, Niedzwiecki A, *et al*. Modulation of u-PA, MMPs and their inhibitors by a novel nutrient mixture in pediatric human sarcoma cell lines. Int J Oncol, 2013, 43: 1027–1035.
9. Kim RK, Kim MJ, Seong KM, *et al.* Beneficial effects of low dose radiation in response to the oncogenic KRAS induced cellular transformation. Sci Rep, 2015, 5: 15809.
10. Mitchel RE. Adaption by low dose radiation exposure: a look at scope and limitations for radioprotection. Dose Response, 2015, 13: dose-response.14-025.
11. Zeng G, Day TK, Hooker AM, *et al*. Non-linear chromosomal inversion response in prostate after low dose X-radiation exposure. Mutat Res, 2006, 602: 65–73.
12. Sun WH, Yu HS, Shang QJ. The effect of pre-low-dose X-ray radiation on tumor inhibition of HepG2 cells in tumor-bearing nude mice. Chinese-German J Clin Oncol, 2012, 6: 340–343.
13. Liu J, Yu HS, Shang QJ. The effects of low-dose splenic irradiation and radiotherapy on immune system of patients with locally advanced non-small cell lung cancer. Chinese-German J Clin Oncol, 2012, 2: 51–55.
14. Yu HS, Song AQ, Liu N, *et al*. Effects of low Dose Pre-irradiation on the toxicity of Cyclophosphamide. Chinese-German J Clin Oncol, 2011, 2: 70–76.
15. Song C, Zhu S, Wu C, *et al*. Histone deacetylase (HDAC) 10 suppresses cervical cancer metastasis through inhibition of matrix metalloproteinase (MMP) 2 and 9 expression. J Biol Chem, 2013, 288: 28021–28033.
16. Li HL, Han L, Chen HR , *et al*. PinX1 serves as a potential prognostic indicator for clear cell renal cell carcinoma and inhibits its invasion and metastasis by suppressing MMP-2 via NF-κB-dependent transcription. Oncotarget, 2015, 6: 21406–21420.
17. Han X, Yan DM, Zhao XF, *et al*. GHGKHKNK octapeptide (P-5m) inhibits metastasis of HCCLM3 cell lines via regulation of MMP-2 expression *in vitro* and *in vivo* studies. Molecules, 2012, 17: 1357–1372.

DOI 10.1007/s10330-016-0156-9
Cite this article as: Jia XM, Yu HS. Modulation of MMP-2 and TIMP-2 by low dose radiation in mice bearing S180 sarcoma. Oncol Transl Med, 2016, 2: 127–131.

Oncology and Translational Medicine
DOI 10.1007/s10330-016-0134-z

June 2016, Vol. 2, No. 3, P132–P137

ORIGINAL ARTICLE

Feasibility and reliability of the revised Edmonton Symptom Assessment System (ESAS-r) in Egyptian patients with advanced cancer: A single institutional experience

Dina A. Salem, Azza M. Adel, Ahmed E. Essa, Mohamed O. Alorabi (✉), Zeinab M. Elsayed

Department of Clinical Oncology, Ain Shams University Hospitals, Cairo, Egypt

Abstract

Objective This study aims to test the acceptance, feasibility, and usefulness of the Arabic version of the revised Edmonton Symptom Assessment System (ESAS-r) among Egyptian patients with advanced cancer and to compare the rates of symptoms documented by patients and physicians.

Methods Between August 2014 and February 2015, a total of 140 patients at Ain Shams University Hospitals in Cairo, Egypt received the Arabic version of the ESAS-r. For each patient, the ESAS-r was completed twice, first by the treating physician (as part of the basic assessment) and a second time by the patient, with a maximum of 2 hours between the two assessments. An additional survey was included to assess patients' acceptance of the survey and their preferences.

Results Out of 140 enrolled patients in the study, 11 patients refused to complete the questionnaire, and 10 patients were excluded due to incomplete records in their medical records. Complete data was retrieved for 119 patients who were included for further analyses. The 78 (65%) patients declared that the test was clear and easy to complete. They were able to answer the test without help. Collectively, tiredness and sense of well-being were the most commonly encountered symptoms in ratings obtained by both patients and physicians. Tiredness was the only symptom showing a significant difference between the two rating methods, patient-rated scores being higher (P = 0.032). Cronbach's alpha showed that both tests completed by the physician and the patients were internally consistent: the physician-rated test had a coefficient of 0.877, and the patient-rated test had a coefficient of 0.863. All ESAS scores had good internal consistency, with a Cronbach's alpha coefficient of 0.88. The internal consistency remained high after removal of individual symptom scores, with Cronbach's alpha coefficients ranging from 0.823 to 0.902, indicating that no individual question had undue influence on the total ESAS score.

Conclusion The ESAS-r was easily understood by and applicable to patients. There was no significant discrepancy in the rates of symptoms reported by the patients and physicians, apart from tiredness. Based on this, the test could be applied on a larger scale with in-home patients. This test can be cost-effective and can decrease the number of hospital visits among advanced cancer patients in need of supportive treatment rather than active cancer therapy.

Received: 23 January 2016
Revised: 11 March 2016
Accepted: 25 April 2016

Key words: advanced cancer; palliative care; Egypt; Edmonton Symptom Assessment System (ESAS)

While cancer rates in general are decreasing in the United States and many developed countries, they are increasing in developing and economically struggling countries [1]. Cancers in these regions are much more likely to go undetected until advanced stages and a greater proportion of patients will suffer severe symptoms than in high income countries [2].

Approximately 80% of cancer patients need palliative care and one of the priorities for global cancer research identified by the World Health Organization (WHO) is the development of effective palliative care delivery models [3]. Unfortunately, palliative care in Egypt is in an early stage of development with few palliative care activities available [4] and patients with advanced and end stage

✉ Correspondence to: Mohamed O. Alorabi. Email: Mohamed_Alorabi@med.asu.edu.eg

cancer have to attend by themselves to assess their condition and decide on further treatment. On the other hand, to effectively treat symptoms of this subset of patients, it is important to obtain their opinions directly. When these patients self-report their symptoms, the frequency and severity data for the symptoms tend to vary significantly from those identified by health care providers and from the data recorded in charts and on research forms [5].

The Edmonton Symptom Assessment System (ESAS) is a self-reporting tool of symptom intensity, initially developed for advanced cancer patients. It is designed to enable repeated quantitative measurements of symptom intensity with minimal patient burden [6]. The ESAS includes nine common symptoms of advanced cancer, namely pain, tiredness, nausea, depression, anxiety, drowsiness, appetite, well-being, and shortness of breath, with the option of adding a tenth patient-specific symptom not provided in the questionnaire [7]. In the original version, these nine symptoms were scored using a visual analogue scale (VAS), ranging from 0 to 100 mm with higher scores indicating greater symptom severity and this version has been validated in an outpatient oncology setting [7–8].

The VAS format has since been replaced by a numerical rating scale (NRS) scored between 0 and 10. Ideally, the ESAS is completed by patients. However, if the patient has limitations in completing the questionnaire, then it is completed with the assistance of a caregiver (a family member, friend, or health professional closely involved in the patient's care), with the exception of the more subjective symptoms of fatigue, depression, anxiety, and well-being [9]. The ESAS had been tested and validated after translation into a number of languages, including Spanish, Turkish, Italian, and Arabic [10–13].

The ESAS has some drawbacks that may be related to the cultural background of patients, their care givers and the medical staff. The test may be not easy for some patients to understand and others can be confused or unable to understand terms such as "well-being," "tiredness," and "drowsiness" [14–15]. Another drawback is the discrepancy in the rating of symptoms between the patient and the treating staff (physician or nurse) [8].

Many patients with advanced stage cancer at Department of Clinical Oncology, Ain Shams University Hospitals, Egypt, come from remote areas and the majority of them have economic and logistic problems in transportation. There is no dedicated palliative care unit at our hospital and patients with advanced cancer and in need for palliation are managed in the outpatient clinics. The ESAS can be a useful tool to follow these patients at home and decrease their visits to hospital.

Based on this, we initiated this study to test the reliability of the ESAS-r in regard to inter-rater reliability (physician and patient both completing ESAS at the same time, independently) and internal consistency. Also, we would like to test the acceptance, feasibility, and usefulness of ESAS among Egyptian patients with advanced cancer, and to compare the patient and proxy (physician) assessments, as this is the first time that our patients have completed this questionnaire by themselves.

Patients and methods

Patients

This study was approved by the ethical committee of Ain Shams Faculty of Medicine with exemption from informed consent. Patients with advanced stage cancer receiving treatment at Department of Clinical Oncology, Ain Shams University Hospitals in Cairo, Egypt, between August 2014 and February 2015 were enrolled in this cross-sectional study. Eligibility criteria included patients with metastatic, refractory, or relapsed cancer beyond curative treatment, age ≥ 18 years and intact cognitive function as assessed by the Arabic version of the Mini-Mental State Examination (MMSE) [16]. Patients under palliative radiotherapy or palliative chemotherapy were eligible. Patients were excluded if they had delirium, dementia, uncontrolled psychiatric disease, or symptomatic brain metastases.

Study design

Between August 2014 and February 2015, a total of 140 patients at Ain Shams University Hospitals in Cairo, Egypt received the Arabic version of the revised Edmonton Symptom Assessment System (ESAS-r) [13], which is freely available for use online. For each patient, the ESAS-r was completed twice, first by the treating physician after discussion with the patient (as part of the basic routine assessment) and a second time by the patient, with a maximum of 2 hours between the two assessments to test the inter-rater agreement. In order to examine the acceptance, feasibility, and usefulness, an additional survey was completed by the patients after answering the ESAS-r. It included the following questions. (1) Do you find this test useful for you? (2) Were the questions clear for you? (3) Were you able to answer all the questions without help? (4) Do you prefer to take the test with the help of medical staff or a relative? Patients' demographic data was retrieved from their medical records and ECOG performance status was assessed for each patient by the physician.

Statistical methods

We aimed to test the inter-rater reliability of the test as well as the internal consistency. Inter-rater reliability is the degree of agreement among raters/observers (in our study, the physician and the patient). It was evaluated using a *T*-test. On the other hand, internal consistency

Table 1 Demographic characteristics of the studied patients

Patient characteristics	Number	%
Age (year)		
≤ 55	64	53.8
> 55	55	46.2
Sex		
Male	48	40.3
Female	71	59.7
Primary tumors		
Breast	34	28.6
Female genitourinary	10	8.4
Gastrointestinal tract (GIT)	23	19.3
Lung	21	17.6
Male genitourinary	12	10.1
Carcinoma of unknown primary	19	16.0
Number of metastatic sites		
Single	82	69.0
Two	25	21.0
Three or more	12	10.0
Metastatic site		
Bone	50	42.0
Brain	27	22.7
Liver	29	24.4
Lung	39	32.8
Local recurrence (Breast)	17	14.3
ECOG PS		
≤ 2	69	58.0
> 2	50	42.0

is used to measure the homogeneity of the items of the tested scale and whether the items are highly correlated with each other. Cronbach's alpha test for internal consistency was evaluated for both the patient-rated and physician-rated tests. Standard descriptive statistics, including mean, median, standard deviation, range, proportion, and frequency, together with 95% confidence intervals, were calculated using IBM SPSS Statistics (V. 21.0, IBM Corp., USA, 2012).

Results

Out of 140 enrolled patients in the study; 11 patients refused to complete the questionnaire. Main causes for refusal were frustration and thinking their condition was hopeless. Some patients were unable to wait 2 hours to retake the test, being dependent on other relatives / care providers to take them home, an understandable issue considering the serious mobility limiting factors in such patients. Ten cases were excluded due to incomplete data in their medical records. Complete data was retrieved from 119 patients who were included for further analyses. A total of 90 patients were interviewed in the outpatient clinic, and 29 patients were interviewed in the inpatient unit.

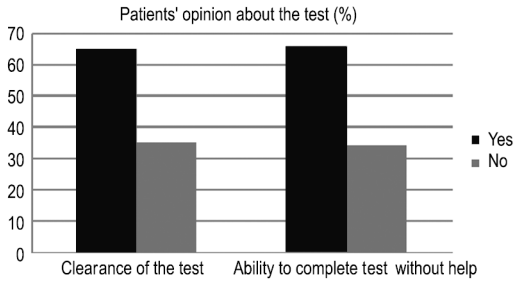

Fig. 1 Patients' opinion about the test

Patients' characteristics

Regarding the demographic data of the patients (Table 1), seventy-one (59.7%) were females, the median age was 50 years (range from 20–84 years), the most common primary tumor was breast tumor (28.6%) followed by lung tumor (19.3%). Eighty-two (69%) patients had a single site of metastasis while 25 (21%) patients had two metastatic sites and the remaining 12 (10%) patients had ≥ 3 metastatic sites. Bone represented the commonest site of metastasis. Fifty (42%) of the study population patients had ECOG performance status > 2.

Patients' opinions about the test

A total of 99 (83%) patients found the test useful for their medical condition. The majority of the patients (65%) declared that the test was clear. A total of 79 (66%) patients were able to answer the test without help; forty (34%) patients needed assistance from the researcher or a relative to finish the questionnaire, mostly due to illiteracy and their level of education (Fig. 1). The illustration part of the questionnaire was appreciated by the majority of the patients. Only nine (8%) patients reported other symptoms.

Inter-rater reliability

Collectively tiredness and sense of well-being were the most commonly encountered symptoms in ratings obtained by both patients and physicians (Table 2). Tiredness was the only symptom showing a significant difference between the two rating methods, patient-rated scores being higher ($P = 0.032$).

Internal consistency

Cronbach's alpha was then calculated (Table 3), and it was found that both tests performed by the physician and the patients were internally consistent; the physician-rated test had a coefficient of 0.877, and the patient-rated test had a coefficient of 0.863.

All ESAS-r scores had good internal consistency, with a Cronbach's alpha coefficient of 0.88. The internal consistency remained high after removal of individual symptom scores, with Cronbach's alpha coefficients ranging

Table 2 ESAS scores obtained by physician and patient ratings

	Physician		Patients		Independent *t*-test	
	Mean	SD	Mean	SD	*t*	*P*
Pain	4.34	1.68	4.72	2.15	–1.512	0.132
Tiredness	5.07	1.69	5.61	2.12	–2.163	0.032
Drowsiness	2.18	2.09	2.40	2.43	–0.772	0.441
Nausea	3.03	1.74	3.25	1.95	–0.913	0.362
Appetite	4.61	1.85	5.08	2.14	–1.818	0.070
Shortness of breath	2.76	2.24	2.91	2.38	–0.504	0.615
Depression	3.83	2.18	3.97	2.34	–0.459	0.646
Anexiety	4.24	2.17	4.33	2.24	–0.294	0.769
Well-being	5.87	2.00	5.97	2.14	–0.376	0.707
Total score	35.92	12.63	38.23	14.58	–1.302	0.194

Table 3 Cronbach's alpha after removal of individual symptom scores in the ESAS performed by the physician and the patient

ESAS	Cronbach's alpha if item deleted	
	Physician	Patient
Pain	0.850	0.881
Tiredness	0.835	0.867
Drowsiness	0.844	0.880
Nausea	0.854	0.888
Appetite	0.836	0.870
Shortness of breath	0.868	0.902
Depression	0.840	0.873
Anexiety	0.852	0.887
Well-being	0.828	0.863
Other	0.879	N/A

from 0.823 to 0.902, indicating that no individual question had an undue influence on the total ESAS score.

Discussion

To our knowledge, this is the first study to test the ESAS on Egyptian patients with advanced cancer at out-patient oncology clinics outside of a palliative care unit. The ESAS was originally developed and applied in the palliative care setting. Few studies have evaluated the use of the ESAS outside palliative care units or long-term hospice facilities. The trials for using the tools to monitor symptoms for palliative patients in out-patient settings have shown positive results [17–19]. Follwell *et al* used the ESAS in a palliative care outpatient clinic. The administration of the ESAS at the initial assessment, one week, and one month later showed marked improvement in both symptom control and patient satisfaction with care. These results are encouraging for the use of the ESAS to provide enhanced symptom management for patients not requiring inpatient care [20].

The ESAS-r was described as generally clear by 65% of our studied patients while 34% found it confusing to express the severity of the symptoms in numbers and needed assistance. In a pilot study conducted by Baba and colleagues [21], 71% of their 24 patients felt that the ESAS was simple to fill in and there were no missing questions. In another multicenter study, 160 patients were enrolled, and 83% rated the ESAS-r as very easy or easy to understand [17]. However, about 18% of our patients were illiterate, and this could explain the lower figures reported in the current study.

Patient assessment of symptoms is considered the "gold standard" [22–23]. However, there are some situations in which proxy assessments may be helpful or necessary, for example when patients over- or under-report their symptoms, or when they are mildly to moderately disoriented [8].

There is no regular self-assessment of symptoms by patients in our department and symptom assessment is done mainly by the treating physician. Thus, it was important to study the correlation between symptom assessment by both physician and patient. In our study, we compared the results obtained from the questionnaire performed by the physician with that performed by patients in the same setting and circumstances (with a maximum of 2 h between the assessments). The results were comparable with no statistically significant difference in the total score (mean score of 35.92 ± 12.63 and 38.23 ± 14.58 for physician's and patients' completed ESAS-r respectively). Both the tests performed by the physician and the patient showed internal consistency and Cronbach's alpha score for the whole test and individual items showed that all ESAS-r scores had good internal consistency, with a Cronbach's alpha coefficient of 0.88. The internal consistency remained high after removal of individual symptom scores, with Cronbach's alpha coefficients ranging from 0.823 to 0.902, indicating that no individual question had undue influence on the total ESAS-r score. This is in contrast to Nekolaichuk and his colleagues who compared patient and proxy (physician and nurse) assessments of symptoms using ESAS in advanced cancer patients. Their sample included 49 patients with advanced cancer in an acute palliative care facility. Every patient

had three independent assessments on two separate occasions within 11 days of admission. In their study, average physician ratings of symptoms were lower than patient ratings across both occasions [8]. Other studies [24–28] were the work of Nekolaichuk and her colleagues.

In the current study, tiredness score was significantly higher in the patient-rated test; this could indicate an overestimation of tiredness in advanced cancer patients. Hence, when trying to evaluate a case without seeing the patient, the measure of tiredness should be interpreted with caution. Tiredness should not be underestimated, yet it should not be considered the sole item determining whether the patient is scheduled for an urgent visit. In the study of Nekolaichuk *et al*, the physician ratings were significantly lower ($P < 0.01$) for three of the symptoms: drowsiness, shortness of breath, and pain, but not tiredness [8].

We recognize that the use of systematic patient-reported assessment is important to improve palliative care for patients with advanced cancer. Improving symptom management of cancer patients needs training of health care professionals and regular documentation of assessment findings. These changes may be challenging for some already overburdened clinical teams. Nevertheless, it is likely that such changes can be made: our findings suggest that efforts toward incorporating symptom assessment in daily practice should be done because it was found that there was a reasonable association between patient reporting and clinical impressions of the treating physician.

Palliative care of cancer patients is a growing medical specialty in Egypt. There is a need to develop tools and methods that are convenient for Egyptian patients to assess the burden of symptoms as well as special training programs for physicians to improve the quality of health care in different cancer centers.

Conclusion

To our knowledge, this is the first study in Egypt to examine the feasibility of using the ESAS-r for reporting symptoms in patients with advanced stage cancers. The current study showed that self-rating by patients using the ESAS-r was well appreciated by patients, was reliable, and could be applied on a larger scale with in-home patients. This test can be cost-effective for deciding whether to transport patients to hospital versus reporting from home while the patient is actually in need of supportive treatment rather than active cancer therapy. However, more research is necessary to identify the necessary tools for making these assessments in the context of different symptoms and settings and to develop the training needed by health care providers to integrate these tools and the information they yield into their clinical practice.

Conflicts of interest

The authors indicated no potential conflicts of interest.

References

1. Jemal A, Siegel R, Xu J, *et al*. Cancer statistics, 2010. CA Cancer J Clin, 2010, 60: 277–300.
2. Sloan FA, Gelband H, eds. Cancer control opportunities in low-and middle-income countries. National Academies Press, 2007.
3. World Health Organization. National cancer control programmes: policies and managerial guidelines. 2002.
4. Alsirafy SA, El Mesidy SM, Abou-Elela EN. Where do Egyptian palliative care patients with cancer die? Am J Hosp Palliat Care, 2010, 27: 313–315.
5. Davidson SE, Trotti A, Ataman OU, *et al*. Improving the capture of adverse event data in clinical trials: the role of the International Atomic Energy Agency. Int J Radiat Oncol Biol Phys, 2007, 69: 1218–1221.
6. Bruera E, Kuehn N, Miller MJ, *et al.* The Edmonton Symptom Assessment System (ESAS): a simple method for the assessment of palliative care patients. J Palliat Care, 1991, 7: 6–9.
7. Chang VT, Hwang SS, Feuerman M. Validation of the Edmonton Symptom Assessment Scale. Cancer, 2000, 88: 2164–2171.
8. Nekolaichuk CL, Bruera E, Spachynski K, *et al.* A comparison of patient and proxy symptom assessments in advanced cancer patients. Palliat Med, 1999, 13: 311–323.
9. Bruera E, Neumann CM, Gagnon B, *et al*. Edmonton regional palliative care program impact on patterns of terminal cancer care. Canadian Med Asso J, 1999, 161: 290–293.
10. Carvajal A, Hribernik N, Duarte E, *et al*. The Spanish version of the Edmonton Symptom Assessment System-revised (ESAS-r): first psychometric analysis involving patients with advanced cancer. J Pain Symptom Manage, 2013, 45: 129–136.
11. Yeşilbalkan ÖU, Özkütük N, Karadakovan A, *et al*. Validity and reliability of the Edmonton Symptom Assessment Scale in Turkish cancer patients. Turkish J Cancer, 2008, 38: 62–67.
12. Moro C, Brunelli C, Miccinesi G, *et al*. Edmonton symptom assessment scale: Italian validation in two palliative care settings. Support Care Cancer, 2006, 14: 30–37.
13. ESAS-r – Edmonton Zone Palliative Care Program: ESAS-r Arabic v.1: 01-Nov-12 [Internet]. Cancer Care Ontario. 2016 [cited 25 May 2016]. Available from: https://www.cancercare.on.ca/common/pages/UserFile.aspx?fileId=33746.
14. Watanabe S, McKinnon S, Macmillan K, *et al.* Palliative care nurses' perceptions of the Edmonton Symptom Assessment Scale: a pilot survey. Int J Palliat Nurs, 2006, 12: 111–114.
15. Garyali A, Palmer JL, Yennurajalingam S, *et al.* Errors in symptom intensity self-assessment by patients receiving outpatient palliative care. J Palliat Med, 2006, 9: 1059–1065.
16. Al-Rajeh S, Ogunniyi A, Awada A, *et al.* Preliminary assessment of an Arabic version of the Mini-Mental state examination. Ann Saudi Med, 1999, 19: 150–152.
17. Watanabe SM, Nekolaichuk C, Beaumont C, *et al*. A multicenter study comparing two numerical versions of the Edmonton Symptom Assessment System in palliative care patients. J Pain Symptom Manage, 2011, 41: 456–468.
18. Rabow MW, Dibble SL, Pantilat SZ, *et al.* The comprehensive care team: a controlled trial of outpatient palliative medicine consultation. Arch Intern Med, 2004, 164: 83–91.
19. Rummans TA, Clark MM, Sloan JA, *et al.* Impacting quality of life

for patients with advanced cancer with a structured multidisciplinary intervention: a randomized controlled trial. J Clin Oncol, 2006, 24: 635–642.
20. Follwell M, Burman D, Le LW, *et al*. Phase II study of an outpatient palliative care intervention in patients with metastatic cancer. J Clin Oncol, 2009, 27: 206–213.
21. Baba K, Fransson P, Lindh J. Use of a modified ESAS in cancer patients: a pilot study of patient and staff experiences. Int J Palliat Nurs, 2007, 13: 610–616.
22. Portenoy RK, Hagen NA. Breakthrough pain: definition, prevalence and characteristics. Pain, 1990, 41: 273–281.
23. Bruera E, Suarez-Almazor M, Velasco A, *et al.* The assessment of constipation in terminal cancer patients admitted to a palliative care unit: a retrospective review. J Pain Symptom Manage, 1994, 9: 515–519.
24. Söllner W, DeVries A, Steixner E, *et al.* How successful are oncologists in identifying patient distress, perceived social support, and need for psychosocial counselling? Br J Cancer, 2001, 84: 179–185.
25. Palma A, Del Río I, Bonati P, *et al*. Frequency and assessment of symptoms in hospitalized patient with advanced chronic diseases: is there concordance among patients and doctors? Rev Med Chil (Spanish), 2008, 136: 561–569.
26. Ewing G, Rogers M, Barclay S, *et al*. Palliative care in primary care: a study to determine whether patients and professionals agree on symptoms. Br J Gen Pract, 2006, 56: 27–34.
27. Brunelli C, Costantini M, Di Giulio P, *et al.* Quality-of-life evaluation: when do terminal cancer patients and health-care providers agree? J Pain Symptom Manage, 1998, 15: 151–158.
28. Rhondali W, Hui D, Kim SH, *et al.* Association between patient-reported symptoms and nurses' clinical impressions in cancer patients admitted to an acute palliative care unit. J Palliat Med, 2012, 15: 301–307.

DOI 10.1007/s10330-016-0134-z
Cite this article as: Salem DA, Adel AM, Essa AE, *et al*. Feasibility and reliability of the revised Edmonton Symptom Assessment System (ESAS-r) in Egyptian patients with advanced cancer: A single institutional experience. Oncol Transl Med, 2016, 2: 132–137.

Oncology and Translational Medicine
DOI 10.1007/s10330-016-0128-x

June 2016, Vol. 2, No. 3, P138–P141

REVIEW ARTICLE

Progress in research on the relationships among tumor blood supply patterns

Jie Li, Xiaobo Du (✉)

Department of Oncology, Mianyang Central Hospital, Mianyang 621000, China

Abstract

Tumor cell growth, invasion, and metastasis require a blood supply. The diversity of tumor blood supply patterns and the biological properties of tumor cells play important roles in these processes. The discovery of vascular mimicry (VM) has enhanced the understanding of the plasticity of tumor cells and angiogenesis. VM is only a supplemental form of tumor microcirculation. However, the extensive clinical significance and special formation of VM have generated new ideas regarding anti-vascular tumor therapy. Currently, the exploration of the relationship between VM and other blood supply patterns is in the early stages, and many questions remain unanswered. Further in-depth studies of the relationships among tumor blood supply patterns will identify novel anti-tumor therapeutics.

Received: 27 December 2015
Revised: 1 February 2016
Accepted: 25 April 2016

The growth of a tumor requires a blood supply. Recent studies have suggested that the pattern diversity of the tumor blood supply and the biological properties of tumor cells play important roles. It is currently thought that the mode of tumor blood supply may be one of three types: endothelium-dependent vessels, mosaic vessels (MV), or vascular mimicry (VM). The relationships between the three modes of tumor blood supply are not clear and be a focus in numerous future studies.

Tumor blood supply patterns

Endothelium-dependent vessels

Classic angiogenic pathways include vasculogenesis and angiogenesis. Vasculogenesis refers to the differentiation of mesoderm-derived hemangioblastomas into endothelial cells, which line the capillaries and are involved in microcirculation. Angiogenesis refers to the process whereby new blood vessels form from pre-existing vessels and concerns the formation of endothelial cells through division, blastomycosis, expansion, and extension. Tumor angiogenesis involves a variety of cells and molecular interactions, including vascular endothelial basement quality degradation, endothelial cell migration, endothelial cell proliferation, formation of endothelial cell branch pipes, and formation of new vascular rings and basement membranes. Thus, tumor cells and endothelial cells interact throughout the entire process of tumor angiogenesis.

A number of studies have shown that active substances regulate tumor angiogenesis. These substances include a series of growth factors, cytokine polypeptides, low-molecular weight lipids, nucleotides, and vitamins, such as vascular endothelial growth factor (VEGF), fibroblast growth factors, interleukin-1, and interleukin-8 [1–9]. VEGF can directly stimulate endothelial cell migration, proliferation, and division, as well as increase microvascular permeability, which plays an important role in tumor angiogenesis [10–11]. Moreover, the coordination of angiogenesis inhibitors is involved in the process. Under normal conditions, equilibrium exists between excessive angiogenesis and inhibition of vascular degeneration [12–13].

Vascular mimicry

VM is the generation of microvascular channels without the participation of endothelial cells. In 1999, Maniotis *et al* [14] reported VM for the first time in their study of melanoma. The expression of VM was observed by immunohistochemical double staining of CD31 and by periodic acid-Schiff staining. Vascular endothelial cells stained by the endothelial cell marker CD31 were positive in tumor tissues, and the VM vessel wall was surrounded by tumor cells without vascular endothelial cells; thus, CD31 was marked as negative. The extracellular matrix stained

✉ Correspondence to: Xiaobo Du. Email: duxiaobo2005@126.com

using the periodic acid-Schiff reaction in the VM vessel wall, combined with hematoxylin and eosin staining, can detect the expression of the VM. Vascular mimicry can be described as follows: the vessel wall, which lacks endothelial cells, is arranged around the tumor cells; although blood flows through the vessel, there is no obvious inflammatory cell infiltration or surrounding necrosis. VM involves the interconnection of normal tumor blood vessels to provide a blood supply to the tumor tissue, indicating its functional role in microcirculation. The presence of VM in a variety of malignant tumors was subsequently confirmed [15–19]. In most studies, the expression of VM was an adverse factor in patient prognosis.

The mechanism for the formation and regulation of VM in blood vessels has been of great interest in tumor research in recent years. Based on a series of studies on melanoma, Hess *et al* [20] proposed a molecular signaling pathway for the regulation of VM formation. They considered a variety of factors associated with VM, such as epithelial cell kinase (EphA2), vascular endothelial cadherin, focal adhesion kinase (FAK), extracellular signal-regulated kinases 1 and 2, phosphoinositide 3-kinase (PI3K), and matrix metalloproteinase (MMP), all of which are associated with the mechanism of VM formation. Furthermore, Lu *et al* [21] reported that the formation of VM was increased in highly invasive gallbladder cancer cells via the PI3K/MMPs/Ln-5γ2 and/or the EphA2/FAK/Paxillin signaling pathways. This provides new targets for the treatment of human gallbladder cancer. However, studies of the mechanism of VM are problematic and researchers have reported a variety of factors that regulate VM formation. Comito *et al* [22] showed that the production of mitochondrial reactive oxygen species enhances hypoxia inducible factor-1α stability, leading to the activation of Met oncogenes. This in turn leads to the formation of metastatic melanoma cells and an increase in the ability to form VM. In a study of ovarian cancer, Millimaggi *et al* [23] found that the formation of CD147 and VM are correlated. CD147 is highly expressed in tumor cells in VM, and the expression of CD147 in ovarian cancer cell lines was found to be correlated with tumor invasiveness. The treatment of SKOV3 cells (a cancer cell line with high invasion activity) with small interfering RNA against CD147 significantly suppressed the ability of these cells to generate non-endothelial channels; however, transfection of CD147 cDNA into the CABA I cell line (a line with low invasion activity) resulted in increased tumor invasiveness and enabled the formation of vascular channels. Sun *et al* [24], in the detection of Twist1 expression in human hepatocellular carcinoma samples and cell lines, found overexpression of Twist1 in VM positive expression in hepatoma cells, and associated this result with the formation of VM. In summary, the formation of VM is induced by several factors functioning in concert and is the result of gene inversion, tumor cell plasticity, effect of protein molecular biology, and environment.

Mosaic vessels

The MV pattern is a special type of tumor blood supply that represents the transition mode between endothelial vascular dependence and vasculogenic mimicry. The vascular walls of MVs are composed of endothelial cells and tumor cells,which differ from the endothelium-dependent vascular system and vasculogenic mimicry.The mechanism of formation may be related to the formation of tumor vascular endothelial cells. Large gaps appear in the vessel wall by the shedding of endothelial cells; and these enable cancer cells exposed to the lumen and participated in blood vessel formation. Studies have shown that there is some loss of immune marker activity in endothelial cells during the tumor evolution process [26–28]. Zhou *et al* [29] showed that a large proportion of mosaic areas vary depending on their location, but most are areas of low collagen IV and laminin immunoreactivity. This suggests that the mechanism of MV formation involves extensive loss of the basement membrane. Given the lack or degradation of the basement membrane, which provides mechanical support to the vessel wall and acts as a physiological barrier, cancer cells can directly contact the vessel wall. This leads to the "mosaic" phenomenon between tumor cells and endothelial cells. Cao [30] showed that tissue present during early MV formation was disorganized and showed a lack of clear separation between arterioles and venules, lack of appropriate coating of mural cells, and high permeability. Therefore, further studies on MV will aid anti-angiogenic therapy.

Relationship between VM and other tumor blood supply patterns

The growth of solid tumors is inseparable from the blood supply. Folkman [31], known as the father of angiogenesis, proposed the classical theory of tumor angiogenesis. According to this theory, a tumor with a volume of less than 2–3 mm^3 can rely on diffusion to obtain adequate nutrition, but when the tumor mass exceeds 2–3 mm^3 endothelial cells are required to build blood vessels for blood supply, otherwise, the tumor will remain dormant or degrade. VM exists as a complement to the tumor blood supply in the form of vessels lined with endothelial cells; the two act together to provide an oxygen supply for tumor growth. A study by Hendrix *et al* [32] found three modes of tumor microcirculation; MV may represent an intermediate stage between VM and endothelium-dependent vessels. Sun *et al* [33–34] confirmed that different stages of tumor growth correspond to different stages in a three-stage process of blood supply patterns. In the early stage of tumor growth, blood is mainly supplied from vascular

mimicry; with increasing tumor volume, endothelial cells continue to proliferate and mosaic vessels appear between the VM and endothelium-dependent blood vessels. The first two are composed of endothelial cells, which gradually replace blood vessels and become the main form of tumor blood supply to provide sufficient blood and oxygen to support tumor growth, invasion, and metastasis. Xiang *et al* [35] also confirmed that VM was generated during the early stage in non-small cell lung carcinoma. As the disease progresses, VM may be replaced by vascular endothelial cells, and thus late-stage patients, particularly those with distant metastases, show fewer VM.

Tumor cells may express angiogenic factors, accumulate normal endothelial cells to form vascular channels, and support tumor growth and spread. However, VM and MV differ from the traditional angiogenesis model. The VM wall is composed of tumor cells and/or basement membrane lining without endothelial cells. In MV, the inner wall can be composed of endothelial cells and tumor cells. In a study examining the number of glioma polyploid giant cancer cells associated with vasculogenic mimicry formation and tumor grade in human glioma, Qu *et al* [36] found that there was more VM and MV in high-grade gliomas than in low-grade gliomas. Additionally, polyploid giant cancer cells generating erythrocytes contribute to the formation of VM and MV. Zhang *et al* [37], using C57 mouse melanoma B16 transplanted tumor tissue, attempted to identify the type of tumor blood supply vessels in different melanoma growth stages. They showed that in the early stage of rapid growth, VM is the dominant form of tumor blood supply. With increasing tumor volume, the number of vasculogenic mimicry channels decreased while the number of endothelium-dependent vessels increased, but the number of mosaic vessels was not associated with tumor size. Finally, endothelium-dependent vessels, which constitute the main pattern of blood supply, increased gradually.

Prospects

The discovery of VM has enriched the knowledge of the plasticity of tumor cells and angiogenesis. However, VM cannot replace endothelial-dependent angiogenesis in tumors, which is the dominant mode, and is only a supplemental form of tumor microcirculation. Nevertheless, the extensive clinical significance and special formation of VM have generated new avenues for anti-vascular tumor therapy. Currently, studies of the relationship between VM and other blood supply patterns are in the early stages. The use of anti-angiogenesis of endothelial vascular-targeted drugs alone have not got any outstanding effect. Anti-VM drugs can be used to compensate for the shortage. However, additional basic research studies are necessary to explore the VM formation mechanism further in order to identify the optimal target and inhibit the formation of VM as well as to develop clinical treatments. Large advances in the field of anti-tumor therapeutics are expected.

Conflicts of interest

The authors indicated no potential conflicts of interest.

References

1. Ranjan A, Bane SM, Kalraiya RD. Glycosylation of the laminin receptor (α3β1) regulates its association with tetraspanin CD151: impact on cell spreading, motility, degradation and invasion of basement membrane by tumor cells. Exp Cell Res, 2014, 322: 249–264.
2. Pahwa S, Stawikowski MJ, Fields GB. Monitoring and inhibiting MT1-MMP during cancer initiation and progression. Cancers (Basel), 2014, 6: 416–435.
3. Samples J, Willis M, Klauber-Demore N.Targeting angiogenesis and the tumor microenvironment. Surg Oncol Clin N Am, 2013, 22: 629–639.
4. Park DJ, Yoon C, Thomas N, *et al*. Prognostic Significance of Targetable Angiogenic and Growth Factors in Patients Undergoing Resection for Gastric and Gastroesophageal Junction Cancers. Ann Surg Oncol, 2013 Dec 27. [Epub ahead of print]
5. Ren T, Qing Y, Dai N, *et al*. Apurinic/apyrimidinic endonuclease 1 induced upregulation of fibroblast growth factor 2 and its receptor 3 induces angiogenesis in human osteosarcoma cells. Cancer Sci, 2014, 105: 186–194.
6. Sayed-Ahmed MM, Hafez MM, Al-Shabanah OA, *et al.* Increased expression of biological markers as potential therapeutic targets in Saudi women with triple-negative breast cancer. Tumori, 2013, 99: 545–554.
7. Pu D, Hou M. Advanced research of fibroblast growth factor receptor in non-small cell lung cancer. Chin J Lung Cancer, 2013, 16: 609–614.
8. Wróbel T, Mazur G, Dzietczenia J, *et al.* VEGF and bFGF gene polymorphisms in patients with non-Hodgkin's lymphoma. Biomed Res Int, 2013, 2013: 159813.
9. Weng WT, Huang SC, Ma YL. α-Melanocyte-Stimulating Hormone Inhibits Angiogenesis through Attenuation of VEGF/VEGFR2 Signaling Pathway. Biochim Biophys Acta, 2014, 1840: 1850–1860.
10. Mauriz E, Carbajo-Pescador S, Ordoñez R, *et al*. On-line surface plasmon resonance biosensing of vascular endothelial growth factor signaling in intact-human hepatoma cell lines. Analyst, 2014, 139: 1426–1435.
11. Croci DO, Cerliani JP, Dalotto-Moreno T, *et al.* Glycosylation-dependent Lectin-receptor interactions preserve angiogenesis in anti-VEGF refractory tumors. Cell, 2014, 156: 744–758.
12. Gupta A, Zhou CQ, Chellaiah MA.Osteopontin and MMP9: associations with VEGF expression/secretion and angiogenesis in PC3 prostate cancer cells. Cancers (Basel), 2013, 5: 617–638.
13. Ripoll GV, Garona J, Pifano M, *et al*. Reduction of tumor angiogenesis induced by desmopressin in a breast cancer model. Breast Cancer Res Treat, 2013, 142: 9–18.
14. Maniotis AJ, Folberg R, Hess A, *et al.* Vascular channel formation by human melanoma cells *in vivo* and *in vitro* vasculogenic mimicry. Am J Pathol, 1999, 155: 739–752.
15. El Hallani S, Boisselier B, Peglion F, *et al.* A new alternative mechanism in glioblastoma vascularization: tubular vasculogenic mimicry.

Brain, 2010, 133: 973–982.
16. Wang SY, Ke YQ, Lu GH, *et al.* Vasculogenic mimicry is a prognostic factor for postoperative survival in patients with glioblastoma. J Neurooncol, 2013, 112: 339–345.
17. Larson AR, Lee CW, Lezcano C, *et al*. Melanoma spheroid formation involves laminin-associated vasculogenic mimicry. Am J Pathol, 2014, 184: 71–78.
18. Chai DM, Bao ZQ, Hu JG, *et al*. Vasculogenic mimicry and aberrant expression of HIF-lα/E-cad are associated with worse prognosis of esophageal squamous cell carcinoma. J Huazhong Univ Sci Technolog Med Sci, 2013, 33: 385–391.
19. Lin P, Wang W, Sun BC, *et al.* Vasculogenic mimicry is a key prognostic factor for laryngeal squamous cell carcinoma: a new pattern of blood supply. Chin Med J (Engl), 2012, 125: 3445–3449.
20. Hess AR, Margaryan NV, Seftor EA, *et al.* Deciphering the signaling events that promote melanoma tumor cell vasculogenic mimicry and their link to embryonic vasculogenesis: role of the Eph receptors. Dev Dyn, 2007, 236: 3283–3296.
21. Lu XS, Sun W, Ge CY, *et al*. Contribution of the PI3K/MMPs/Ln-5γ2 and EphA2/FAK/Paxillin signaling pathways to tumor growth and vasculogenic mimicry of gallbladder carcinomas. Int J Oncol, 2013, 42: 2103–2115.
22. Comito G, Calvani M, Giannoni E, *et al*. HIF-1α stabilization by mitochondrial ROS promotes Met-dependent invasive growth and vasculogenic mimicry in melanoma cells. Free Radic Biol Med, 2011, 51: 893–904.
23. Millimaggi D, Mari M, D' Ascenzo S, *et al.* Vasculogenic mimicry of human ovarian cancer cells: role of CD147. Int J Oncol, 2009, 35: 1423–1428.
24. Sun T, Zhao N, Zhao XL, *et al*. Expression and functional significance of Twist1 in hepatocellular carcinoma: its role in vasculogenic mimicry. Hepatology, 2010, 51: 545–556.
25. Liu J, Huang J, Yao WY, *et al*. The origins of vacularization in tumors. Front Biosci (Landmark Ed), 2012, 17: 2559–2565.
26. di Tomaso E, Capen D, Haskell A, *et al*. Mosaic tumor vessels: cellular basis and ultrastructure of focal regions lacking endothelial cell markers. Cancer Res, 2005, 65: 5740–5749.
27. Dennie CJ, Veinot JP, McCormack DG, *et al.* Intimal sarcoma of the pulmonary arteries seen as a mosaic pattern of lung attenuation on high-resolution CT. AJR Am J Roentgenol, 2002, 178: 1208–1210.
28. Chang YS, di Tomaso E, McDonald DM, *et al*. Mosaic blood vessels in tumors: frequency of cancer cells in contact with flowing blood. Proc Natl Acad Sci U S A, 2000, 97: 14608–14613.
29. Zhou F, Liang LJ, Peng BG, *et al*. Distribution and structure characteristics of mosaic vessels in hepatocellular carcinoma tumor. Chin J Exp Surg, 2008, 25: 826–828.
30. Cao Y. Tumor angiogenesis and molecular targets for therapy. Front Biosci (Landmark Ed), 2009, 14: 3962–3973.
31. Folkman J. Angiogenesis in cancer, vascular, rheumatoid and other disease. Nat Med, 1995, 1: 27–31.
32. Hendrix MJ, Seftor EA, Hess AR, *et al.* Vasculogenic mimicry and tumor-cell plasticity: lessons from melanoma. Nat Rev Cancer, 2003, 3: 411–421.
33. Sun B, Zhang D, Zhang S, *et al.* Hypoxia influences vasculogenic mimicry channel formation and tumor invasion-related protein expression inmelanoma. Cancer Lett, 2007, 249: 188–197.
34. Sun B, Zhang S, Zhang D, *et al*. Vasculogenic mimicry is associated with high tumor grade, invasion and metastasis, and short survival in patients with hepatocellular carcinoma. Oncol Rep, 2006, 16: 693–698.
35. XG Lu, Xiao Li, Fangzhen Shen, *et al*. Vasculogenic mimicry in non-small cell lung cancer and its relationship with tumor stage. Chinese-German J Clin Oncol, 2014, 13: 207–211.
36. Qu Y, Zhang L, Rong Z, *et al.* Number of glioma polyploid giant cancer cells (PGCCs) associated with vasculogenic mimicry formation and tumor grade in human glioma. J Exp Clin Cancer Res, 2013, 32: 75.
37. Zhang SW, Guo H, Zhang DF, *et al*. Preliminary Studies on the Correlation between Time and Three Mod Of Blood Supply in Melanoma Tissues. Chin J Clin Oncol, 2007, 34: 96–99.

DOI 10.1007/s10330-015-0128-x
Cite this article as: Li J, Du XB. Progress in research on the relationships among tumor blood supply patterns. Oncol Transl Med, 2016, 2: 138–141.

Oncology and Translational Medicine

Aims & Scope

Oncology and Translational Medicine is an international professional academic periodical. The Journal is designed to report progress in research and the latest findings in domestic and international oncology and translational medicine, to facilitate international academic exchanges, and to promote research in oncology and translational medicine as well as levels of service in clinical practice. The entire journal is published in English for a domestic and international readership.

Supervised by

Ministry of Education of the People's Republic of China.

Administered by

Tongji Medical College, Huazhong University of Science and Technology.

Submission information

Manuscripts should be submitted to:
http://otm.tjh.com.cn
dmedizin@sina.com

Subscription information

ISSN edition: 2095-9621
CN: 42-1865/R

■ Subscription rates
Subscription may begin at any time. Remittances made by check, draft or express money order should be made payable to this journal. The price for 2015 is as follows: US $ 30 per issue; RMB ￥28.00 per issue.

Database

Oncology and Translational Medicine is abstracted and indexed in EMBASE, Index Copernicus, Chinese Science and Technology Paper Citation Database (CSTPCD), Chinese Core Journals Database, Chinese Journal Full-text Database (CJFD), Wanfang Data; Weipu Data; Chinese Academic Journal Comprehensive Evaluation Database.

Business correspondence

All matters relating to orders, subscriptions, back issues, offprints, advertisement booking and general enquiries should be addressed to the editorial office.

Mailing address
Editorial office of
Oncology and Translational Medicine
Tongji Hospital
Tongji Medical College
Huazhong University of Science and Technology
Jie Fang Da Dao 1095
430030 Wuhan, China
Tel.: +86-27-83662630
Fax: +86-27-83662645
Email: dmedizin@tjh.tjmu.edu.cn

Printer
Changjiang Spatial Information Technology Engineering Co., Ltd. (Wuhan) Hangce Information Cartorgraphy Printing Filial, Wuhan, China
Printed in People's Republic of China